JOURNAL OF PETROLOGY | VOLUME 41 | NUMBER 2 | PAGES 229–256 | 2000

Oxygen Isotope Geochemistry of Oceanic-Arc Lavas

JOHN M. EILER[1]*, ANTHONY CRAWFORD[2], TIM ELLIOTT[3], KENNETH A. FARLEY[1], JOHN W. VALLEY[4] AND EDWARD M. STOLPER[1]

[1]DIVISION OF GEOLOGICAL AND PLANETARY SCIENCES, CALIFORNIA INSTITUTE OF TECHNOLOGY, PASADENA, CA 91125, USA

[2]DEPARTMENT OF GEOLOGY, UNIVERSITY OF TASMANIA, GPO BOX 252C, HOBART, TAS. 7001, AUSTRALIA

[3]FACULTEIT AARDWETENSCHAPPEN, VRIJE UNIVERSITEIT, DE BOELELAAN 1085, 1081 HV AMSTERDAM, NETHERLANDS

[4]DEPARTMENT OF GEOLOGY AND GEOPHYSICS, UNIVERSITY OF WISCONSIN, MADISON, WI 53706, USA

RECEIVED NOVEMBER 2, 1998; REVISED TYPESCRIPT ACCEPTED JULY 15, 1999

Variations of oxygen isotope ratios in arc-related lavas can constrain the contributions of subducted crustal igneous rocks, sediments, and fluids to the sub-arc mantle. We have measured oxygen isotope ratios in 72 arc and back-arc lavas from five ocean–ocean subduction zone systems using laser-fluorination analyses of olivine and other phenocrysts and glass. Eighty percent of our samples have $\delta^{18}O$ values for any given phase (olivine, plagioclase, glass, or biotite) within 0·2‰ of the average value for that phase in upper-mantle peridotites and mid-ocean ridge basalt (MORB); the range for each phase is $\leq 1{\cdot}0$‰. This result contrasts with previous studies of whole-rock samples (which are significantly more variable even after exclusion of samples believed to be altered or fractionated by magmatic differentiation) and demonstrates that most arc-related lavas contain ≤ 1–2% of ^{18}O-enriched crustal oxygen from any source (i.e. assimilation or subducted contributions). Elevations in $\delta^{18}O$ that do occur in these basic, arc-derived magmas relative to values most common for mantle-derived lavas are associated both with 'enriched' radiogenic isotope signatures and, even more strongly, with chemical indices consistent with high integrated extents of melting of their peridotite sources. We interpret these relationships as evidence that melting in the sources of the high-$\delta^{18}O$ lavas we have studied was fluxed by addition of high-$\delta^{18}O$ aqueous fluid (or perhaps a hydrous melt) from the subducted slab, such that sources that contain relatively large components of slab-derived fluid or melt are both relatively ^{18}O enriched and also experienced relatively large amounts of melting. We have developed a quantitative model linking the amount of melting to the extents of ^{18}O, radiogenic isotope, and trace-element enrichment in a mantle source being fluxed by addition of aqueous fluid. Comparison of this model with observed variations in the geochemistry of lavas from the Vanuatu–Fiji–New Caledonia region (the suite of related samples showing the greatest range in $\delta^{18}O$ observed in this study) constrains the amounts and chemical and isotopic compositions of slab-derived phases in the sources of these arc-related lavas. Assuming a $\delta^{18}O$ value of 20‰ for the slab-derived fluid, 0·5–1·0 wt % is added to the sources of most mantle-derived arc magmas; the maximum amount of slab-derived flux in the sources of arc magmas according to our results is 2·5 wt %.

KEY WORDS: *oxygen isotopes; arc volcanism*

INTRODUCTION

There is considerable evidence that igneous rocks, sediments, and fluids from subducted oceanic crust contribute to the formation of convergent margin magmas (e.g. Morris & Tera, 1989; McCulloch & Gamble, 1991; Stolper & Newman, 1994; Elliott *et al.*, 1997; Hawkesworth *et al.*, 1997). These contributions are generally assumed to be introduced into the overlying mantle wedge as aqueous fluids and/or silicate melts released

*Corresponding author.

from the downgoing slab as it heats up. Mixing of these water-rich fluids and melts with peridotite in the overlying mantle leads to the production of magmas with the distinctive petrology and geochemistry of convergent margin igneous rocks. Given the likely thermal structure of the subducting slab and overlying mantle, melting in the mantle wedge may in many cases require and/or be controlled by the introduction of these water- and incompatible-element-rich fluids and/or melts because they significantly lower the temperature of the peridotite solidus (Kushiro *et al.*, 1968).

Efforts to identify and characterize the contributions of subducted materials to arc volcanism have emphasized the abundances and isotopic ratios of minor and trace elements that are relatively abundant in altered basaltic rocks and sediments and are concentrated into aqueous fluids and silicate melts relative to residual solids (e.g. K, B, Sr, U; Morris & Tera, 1989; Plank & Langmuir, 1993; Hawkesworth *et al.*, 1994; Leeman *et al.*, 1994; Ryan *et al.*, 1995). These elements can be sensitive indicators of the presence of slab-derived components in the sources of arc lavas; they can also be used to discriminate among and characterize various slab-derived components (e.g. aqueous fluids vs silicate melts; Elliott *et al.*, 1997) and to estimate the time required for these components to travel from the slab to the source regions of magmas in the mantle wedge (Hawkesworth *et al.*, 1997; Regelous *et al.*, 1997). However, such elements are poor monitors of the absolute amounts of slab-derived components in magmatic sources because the concentrations of these elements vary widely among subducted crustal rocks and sediments (Plank & Langmuir, 1998) and because the partitioning of these elements among minerals, melts, and aqueous fluids is strong, highly variable, and only partially constrained by experiment (Green, 1994; Brenan *et al.*, 1995; Keppler, 1996; Johnson & Plank, 1999).

Oxygen isotopes can provide constraints on the sources of arc volcanism that are complementary to those of trace element abundances and their isotope ratios. Most ultramafic rocks and inferred sources of basaltic lavas have $\delta^{18}O$ [$\delta^{18}O = ({}^{18}O/{}^{16}O_{sample}/{}^{18}O/{}^{16}O_{VSMOW} - 1) \times 1000$, where ${}^{18}O/{}^{16}O_{VSMOW} = 0{\cdot}0020052$] values of $5{\cdot}5 \pm 0{\cdot}2‰$ (Mattey *et al.*, 1994). In contrast, $\delta^{18}O$ values of altered basalts in the uppermost oceanic crust are typically $+10$–$20‰$ (compared with values of 0–7‰ for the lower oceanic crust; Muehlenbachs, 1986; Staudigel *et al.*, 1995); values for coarse clastic sediments are also typically $+10$–$20‰$ (Arthur *et al.*, 1983); values for oceanic clays are typically $+15$–$20‰$ (Arthur *et al.*, 1983); and typical values for carbonate-rich and siliceous pelagic sediments are $+30$–$35‰$ (Kolodny & Epstein, 1976; Arthur *et al.*, 1983). The oxygen isotopic contrast between upper oceanic crust (i.e. sediments and altered basalts) on the one hand and typical upper mantle on the other therefore provides a potential indicator of the presence of subducted upper oceanic crustal materials in the sources of subduction-zone lavas (note, however, that the contrast in oxygen isotope ratios between the mantle and lower-crustal materials may be more subtle and in the opposite direction; Muehlenbachs, 1986). It is known that the distinctive $\delta^{18}O$ values of the oceanic crust can be preserved to depths of tens of kilometers in subduction zones (Bebout & Barton, 1989), can persist for long times in deeply recycled materials (Garlick *et al.*, 1971), and can survive transport through the sub-arc mantle in a melt or fluid phase (Eiler *et al.*, 1998). Moreover, there are only modest variations in the concentration of oxygen in most geological solids and fluids, and the isotopic composition of oxygen is only weakly and predictably fractionated by high-temperature exchange among solids, melts, and fluids (e.g. Chiba *et al.*, 1989; Palin *et al.*, 1996); therefore, variations in oxygen isotope ratios in arc-related magmas may more strongly constrain the absolute amounts of slab-derived components contributing to the mantle sources of arc-related magmas than do incompatible trace elements and their isotopes, i.e. uncertainties in such estimates should stem only from uncertainties of a factor of ~ 2 in the $\delta^{18}O$ values of subducted upper-crustal materials, rather than from uncertainties of an order of magnitude or more in the abundances of incompatible trace elements. Such constraints on the amounts of fluid and/or melt added to the sources of arc lavas could in turn help to constrain the concentrations of incompatible trace elements in the slab-derived components, to distinguish between metasomatic fluids and melts (which may differ substantially in their abundances of certain elements relative to oxygen), and to define the processes by which slab-derived components interact with the mantle (e.g. bulk mixing, chromatographic exchange, fluid-driven melting).

The oxygen isotope geochemistry of arc-related lavas is known principally through measurements of whole-rock samples of andesite and more evolved rocks [see review by Harmon & Hoefs (1995)]. Such data are the basis of several early and fundamental constraints on subduction-related volcanism, including the discovery of the approximate (± 1–$2‰$) correspondence between arc-related andesites on the one hand and peridotites and basalts from other tectonic settings on the other (suggesting an origin of the parental liquids of andesitic magmas by melting of peridotite rather than by direct melting of subducted crustal rocks—a significant finding at the time it was made; e.g. Matsuhisa *et al.*, 1973) and of the importance of crustal assimilation and large-scale crustal melting in arc magmatism (e.g. Hildreth & Moorbath, 1988; Davidson & Harmon, 1989). However, the oxygen isotope ratios of the abundant evolved lavas from arcs have been modified from primitive, mantle-derived values by magmatic processes (e.g. fractional crystallization and crystal accumulation; Woodhead *et al.*,

1987; Harmon & Hoefs, 1995), and fine-grained and glassy lavas are particularly susceptible to subsolidus alteration (Davidson & Harmon, 1989; Harmon & Hoefs, 1995). These high-level fractionation and alteration processes can produce shifts in $\delta^{18}O$ of $\sim$1‰ or greater in lavas and thus hinder the study of the smaller (<1‰) variations in oxygen isotope ratios known to characterize the mantle sources of ocean-island basalts (OIB) (Eiler *et al.*, 1996) and that might be more typical consequences of the interactions of the sub-arc mantle with fluids or melts from the subducted slab. Previous efforts to circumvent these difficulties in applying oxygen isotope geochemistry to the study of arc magmatism have included correction or exclusion of measured $\delta^{18}O$ values of whole-rock specimens inferred to be significantly altered and/or unusually evolved (Woodhead *et al.*, 1987; Davidson & Harmon, 1989; Harmon & Hoefs, 1995), or analysis of glass (Ito & Stern, 1985; Macpherson & Mattey, 1997) or phenocrysts (Singer *et al.*, 1992; Smith *et al.*, 1996; Thirlwall *et al.*, 1996; Macpherson & Mattey, 1997; Macpherson *et al.*, 1998) rather than whole rocks.

We describe in this paper the results of a study of oxygen isotope variations in relatively magnesian lavas from oceanic arcs (and associated back-arc basins) based primarily on measurements on olivine phenocrysts, supported with less extensive measurements on other phenocryst phases and glass. Olivine has a low rate of oxygen exchange in the absence of replacement by alteration minerals (Reddy *et al.*, 1980); it is an early phase in the low-pressure crystallization sequences of primitive basaltic liquids; and it is thought to be present as a major phase in the mantle sources of basalts. It is therefore an obvious target for providing insights into the upper-mantle sources of basic magmas. We note, however, that our emphasis on olivine-bearing lavas may have prejudiced our sampling against magmas (and their fractionation products) produced by single-stage melting of non-ultramafic sources (e.g. partial melts of subducted crust unmodified by reaction with the mantle wedge in transit to the surface), if such magmas exist (Defant & Drummond, 1990). Approximately 20 laser-fluorination measurements of the $\delta^{18}O$ of olivines from arc-related magmas have been previously published, distributed among four studies of the Lau basin, the Lesser Antilles, and the Kermadec–Hikurangi margin (Smith *et al.*, 1996; Thirlwall *et al.*, 1996; Macpherson & Mattey, 1997; Macpherson *et al.*, 1998). We have not integrated these data with our study because of both the small number and wide distribution of these previous measurements and the difficulty in interpreting small (several tenths of per mil) variations in $\delta^{18}O$ measurements from different laboratories without careful cross-standardization. However, we note that data from those studies are generally within the range of results presented here. Results for other phases (glass and clinopyroxene) from these recent studies will be discussed further below.

SAMPLES AND ANALYTICAL METHODS

The suite of samples we have studied includes 72 basalts, basaltic andesites, shoshonites, boninites, and alkali basalts from five ocean–ocean subduction systems: the Mariana arc and back-arc trough, the South Sandwich arc and associated Scotia Sea back arc, the Vanuatu–Fiji arc and nearby New Caledonia arc (these are treated as a single suite in much of the subsequent discussion), and Papua New Guinea [alkaline lavas of the Tabar, Lihir, Tanga, and Feni ('TLTF') islands, derived from melting of the mantle wedge of a recently active subduction zone]. The sample suite was restricted to lavas from oceanic (as opposed to continental) arcs and to olivine-phyric lavas that are more primitive than those typically considered in previous studies of the oxygen isotope geochemistry of arc lavas (the mean MgO and SiO_2 contents of samples for which major element data are available are approximately 7 and 51 wt %), although samples were also chosen so as to include a significant range in minor and trace element geochemistry and radiogenic isotope ratios. Analyses are available for 58 of the 72 samples for major element concentrations, trace element concentrations, mineral chemistry, and/or Sr, Nd, Pb, and/or U-series isotope geochemistry, providing a petrological and geochemical context in which to interpret our data. The supplemental chemical data are reported using the same sample labels as in the literature (Hawkesworth *et al.*, 1977; Saunders & Tarney, 1979; Hawkins & Melchior, 1985; Maillet *et al.*, 1986; Kennedy *et al.*, 1990; Eggins, 1993; Monzier *et al.*, 1993; Sigurdsson *et al.*, 1993; Rogers & Setterfield, 1994; Crawford *et al.*, 1995; Pearce *et al.*, 1995; Elliott *et al.*, 1997; Peate *et al.*, 1997) or are from unpublished studies of A. Crawford or R. Stern; a table including the supporting geochemical data is available on request from the authors. The 14 samples that have not been previously characterized are related to characterized samples and come from previously studied sequences of lavas, such that aspects of their geochemistry can be confidently inferred; these samples are indicated in Table 1 and in the figures. All of the significant variations and trends in $\delta^{18}O$ observed in this study have extremes exhibited by well-characterized samples.

All samples were crushed in a steel percussion mortar and dry-sieved to size fractions of 600–300 μm and 300–150 μm for hand picking of olivine, plagioclase, glass, and/or biotite separates. All separates were cleaned of dust by briefly blowing filtered compressed air over them while holding them in a 100 μm sieve. Olivine

separates were prepared for 67 of the 72 samples; 24 plagioclase separates, 11 glass separates, and two biotite separates were also prepared.

Most mineral and glass separates were analyzed for $\delta^{18}O$ at the CO_2-laser-fluorination laboratory at the University of Wisconsin, Madison ['UW', described in detail by Valley *et al.* (1995)]. A subset of the data was measured by the same methods at the University of Southern California ('USC'). Analyses at UW were made on 12 days over a period of 7 months, whereas those at USC were made on 3 days over a period of 1 month. Measurements of unknowns on each day in both laboratories were accompanied by 4–8 measurements of UWG-2 garnet (Valley *et al.*, 1995) and 2–4 measurements of the SCO-1 olivine working standard (Eiler *et al.*, 1995). The 1σ uncertainty for a given standard on any given day averaged 0·07‰. In addition, 60 of the unknown samples were measured 2–3 times, and the mean of the 1σ uncertainties of these multiple analyses is 0·06‰. On 12 of the 15 days on which analyses were performed, measurements of each standard averaged within 0·1‰ of the accepted value and no systematic correction was applied to the data. On 3 days, however, the averages for both UWG-2 and SCO-1 differed from their accepted values by 0·1–0·2‰, and a correction was applied to the data equal to the average of the differences between the mean-measured value and the accepted value for each of the two standards. Such corrections are required on $\sim$25% of the working days at the UW laboratory and have been inferred to be caused by small variations in the condition of the gas-purification and gas-transfer apparatus (Valley *et al.*, 1995). Four olivine samples (i.e. unknowns) that had been measured on a day on which a correction was applied based on the analyses of the standards were reanalyzed on another day on which no correction was required; the average difference between the corrected and uncorrected measurements was 0·06‰. One analysis of an olivine separate (GUG-3) yielded an anomalous result (3·5‰) that was not reproduced by two further measurements of a new mineral separate from this sample. The anomalous value was discarded, and only the average of two additional measurements is listed in Table 1a.

The accuracy of our analyses was assessed by measurement of seven silicates (three olivines, two basaltic glasses, one biotite, and one plagioclase; Table 1b), six of which had been previously analyzed multiple times by other laboratories using conventional fluorination procedures. The average difference between the mean value of $\delta^{18}O$ for these materials determined by laser fluorination at UW and the accepted values was 0·09‰; that is, comparable with our precision based on repeated analyses of the UWG-2 working standard. Moreover, the UWG-2 garnet standard and three other materials (SCO-1, KHO-1, and AH95-22 glass) were analyzed in both the UW and USC laser fluorination laboratories, and the differences between the average values for these materials from these two laboratories averaged 0·06‰. Overall, these demonstrations of reproducibility and of agreement between laser fluorination analyses at UW and USC and with conventional fluorination analyses allow us to infer that our data are accurate and precise to approximately $\pm$0·07‰ (1σ) for the phases analyzed in this study.

RESULTS

Values of $\delta^{18}O$ determined in this study vary over a range of 1‰ or less for each of the phases analyzed: the ranges are 0·98‰ for the 67 olivine analyses; 0·38‰ for the 24 plagioclase analyses; and 0·14‰ for the 11 glasses (Table 1a). Average values of $\delta^{18}O$ for olivine, plagioclase, and glass are within 0·1‰ of those for fresh mid-ocean ridge basalts (MORBs) or their inferred sources (Ito *et al.*, 1987; Eiler *et al.*, 1996); likewise, the average for olivine in our sample suite is within 0·1‰ of the average for olivine from mantle peridotite xenoliths (Mattey *et al.*, 1994). Even the largest range in $\delta^{18}O$ for a single phase (olivine) is small relative to expectations based on most previous studies of arc-related lavas (Harmon & Hoefs, 1995). The relatively small range in $\delta^{18}O$ is particularly striking given the number and diversity of samples that we have studied: our suite of samples is taken from five different arcs and three back-arc regions and includes much of the range in radiogenic isotope ratios (e.g. $^{87}Sr/^{86}Sr$ = 0·7026–0·7044), trace element compositions (e.g. Ba/Nb = 6–400), U-series radioisotope activity ratios (e.g. $[U^{238}/Th^{230}]$ = 1·0–1·6), and petrologic diversity (i.e. island-arc basalts and basaltic andesites, back-arc-basin basalts, shoshonites, boninites, and alkali basalts) known from oceanic-arc lavas. It should be noted, however, that we have not included any samples characterized by exceptionally high $^{87}Sr/^{86}Sr$ ratios and Th concentrations, such as those common to the Philippines, Indonesia, and the Aeolian islands [i.e. the 'high-Ce/Yb' arcs of Hawkesworth *et al.* (1994)].

Approximately 80% of the $\delta^{18}O$ values for olivine are within the range for typical upper-mantle olivine based on peridotite xenoliths (5·0–5·4‰; Mattey *et al.*, 1994). Only one sample (Charlotte 22 from Vanuatu) is significantly below this range (and this one by only 0·15‰); the remaining $\sim$20% of the samples are enriched in ^{18}O relative to this range by up to 0·43‰ (Fig. 1). Relatively ^{18}O-enriched samples include three island-arc basalts (all from western Vanuatu), three shoshonites (also from the Vanuatu region), three boninites (from Vanuatu and New Caledonia), and six alkali basalts from the TLTF islands (Papua New Guinea). In the following paragraphs we assess some of the systematics of our data, comparisons

Table 1a: Oxygen isotope data and select major elements

Location	Sample	$\delta^{18}O$			SiO_2	MgO	Location	Sample	$\delta^{18}O$			SiO_2	MgO
		Olivine	Glass	Plagioclase					Olivine	Glass	Plagioclase		
Mariana	PAG-2	5·28			49·83	6·20	Vanuatu–Fiji	Tongoa 3	5·45				
arc	URA-5	5·06			53·57	6·13	arc	IH 3	5·21			47·58	8·18
	SAG-1	5·33			53·37	5·57		IH 4	5·21			47·12	11·70
	ARG-1	5·02			51·58	3·04		Tan 3	5·17		5·72	*49·46*	*6·84*
	ARG-2	5·25			50·94	4·98		VL 1	5·24		5·66		
	ARG 4B	5·03		5·68	50·48	4·80		Aoba 1	5·10				
	ARG 8B	5·05			50·50	3·55		Aoba 2	5·18			45·31	22·09
	ALAM-2	(5·25)		5·90	54·95	4·40		Matthew 24C	5·14		5·77	63·11	3·15
	ALAM-5	5·22		5·95	53·39	4·86		Charlotte 22	4·85		5·75	62·83	3·20
	GUG 3	5·09			51·61	3·36		V 11C	5·15			55·76	8·77
	GUG 6	5·03		5·70	51·14	3·99		AR110	5·26		5·66	*48·74*	*5·34*
	GUG 7	5·11			51·02	3·93		Ambrym 28	5·78			51·45	9·16
	GUG 9	5·17			50·99	4·23		Ambrym 68	5·54			49·24	11·68
	GUG 12	4·98		5·96	52·16	3·49		123/3	5·25			47·46	11·75
	GUG 13	5·14		5·69	51·78	3·47							
							Hiyoshi	D54G	5·22			*45·64*	*6·53*
Mariana	WOKD-28	5·02	5·53	5·72	49·95	7·61	shoshonites	D54K	5·09			*45·64*	*6·53*
trough	WOK 16-2	(5·21)	5·57		51·12	7·54	(Marianas)	D54E	5·04			*45·64*	*6·53*
	1832-2	5·28		5·96	55·76	3·87		D54F	5·04			*45·64*	*6·53*
	1833-1	4·96		5·79	53·02	4·60		D54H	5·14		5·68	*45·64*	*6·53*
	1833-11	5·08	5·66	5·68	51·13	7·55		D53F	5·10		5·89	*55·60*	*2·83*
	1846-9	(5·19)	5·55		49·67	6·95		D53E	5·11		5·66	*55·60*	*2·83*
	1846-2	5·30	5·61		50·75	7·00							
							Vanuatu	78/61	5·65			57·17	4·06
South	SSZ-2·1	5·15		5·82	51·25	6·07	boninites	76/35	5·72			52·53	11·50
Sandwich	SSZ-2·2	(5·04)		5·69	51·64	5·67							
arc	SSZ-2·2·5	(5·18)		5·83	*51·64*	*5·67*	New Caledonia	NC52	5·74			57·23	14·30
	SSZ-2·3	5·13		5·72	50·23	6·99	boninite						
Scotia Sea	D20-1	5·35	5·54	6·04	50·58	7·60	Vanuatu/Fiji	Astro 186	5·32			47·92	11·52
back-arc	D20-35	5·23	5·58	5·84	50·58	7·60	shoshonites	Astro 185	5·40			49·36	9·47
	D24-4	5·26	5·61		53·07	6·04		E2d	5·51			48·08	11·47
	D24-6	5·27	5·61		53·07	6·04		E2c	5·75			47·99	9·94
	D23-4	5·40	5·67		50·38	7·33							
	D60-9	5·28	5·66				Tonga–Lihir–	SIM-1	5·55			47·90	14·60
							Tabar–Feni	94AMB-11	5·50				
Vanuatu–Fiji	115/2	5·27			54·66	5·57		TAB-1	5·56				
arc	GM 31	5·27						LIH-2	5·82				
	GA-5	5·01						LIH-6	5·53				
	GB30B	5·20			58·00	4·73		LIH-15	5·32				
	Tongoa 6	5·34			49·42	9·37		LIH-25	5·83				

Italics indicate elemental data based on average values of closely related samples. Parentheses indicate values of $\delta^{18}O$ based on coexisting plagioclase or glass and average plagioclase–olivine or glass–olivine fractionations from this study.

Table 1b: Oxygen isotope standards

Sample	UW	USC	Accepted value
NBS-30 biotite	5·18		5·10
Amelia albite	10·77		10·60*
MK1-8 glass	4·98		5·00†
AH95-22 glass	4·94	4·92	
31-368 olivine	4·79		4·68‡
Brenham olivine	3·49		3·53§
Pavlodar olivine	3·48		3·38§
SCO-1 olivine	5·27	5·20	
KHO-1 olivine	5·32	5·40	

*A. Matthews, personal communication, 1996.
†Garcia *et al.* (1989).
‡Garcia *et al.* (1998).
§Clayton & Mayeda (1996); it should be noted that the ^{17}O correction on these materials does not introduce a significant error in the measurement of $\delta^{18}O$ on CO_2 analyte.

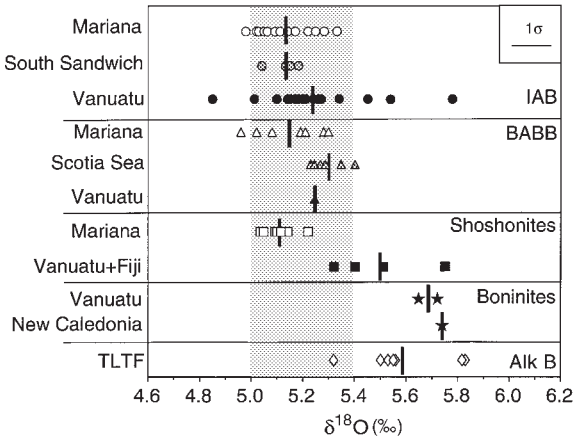

Fig. 1. Values of $\delta^{18}O$ for olivine from oceanic-arc lavas analyzed in this study, organized into groups defined by geographic location and petrologic type. The gray field indicates the range typical of olivine from upper-mantle peridotite xenoliths (Mattey *et al.*, 1994) and inferred for olivine in the MORB source (5·2 ± 0·2‰; Ito *et al.*, 1987; Eiler *et al.*, 1996). Short vertical lines mark average values for each suite of related samples. Samples are labeled by location and by petrologic type: island-arc basalt (IAB, circles), back-arc-basin basalt (BABB, triangles), shoshonite (squares), boninite (stars), and alkali basalt (Alk B, diamonds). TLTF indicates lavas from the Tabar–Lihir–Tanga–Feni islands, Papua New Guinea. Symbols for Mariana arc and back-arc samples are open; for South Sandwich–Scotia Sea samples they are gray; for the Vanuatu–Fiji–New Caledonia suite they are filled; for TLTF samples they are open.

with previous work, and correlations of our data with other geochemical characteristics of the samples.

Distribution of oxygen isotopes among coexisting phases

We have made nine determinations of basaltic glass–olivine oxygen isotope fractionation ($\Delta_{glass-olivine}$; Fig. 2a) and 21 determinations of plagioclase–olivine fractionation ($\Delta_{plagioclase-olivine}$; Fig. 2b; where $\Delta_{i-j} = \delta^{18}O_i - \delta^{18}O_j$). Both of these fractionations are essentially constant given the precision of our measurements: $\Delta_{plagioclase-olivine} = 0{\cdot}65 \pm 0{\cdot}14‰$ (1σ) and $\Delta_{glass-olivine} = 0{\cdot}36 \pm 0{\cdot}11‰$ (1σ). The expected precision of a determination of Δ_{i-j} is 0·10‰ (1σ), based on independent errors of 0·07‰ for a determination of $\delta^{18}O$ on each phase.

The average fractionation we determine between plagioclase and olivine phenocrysts compares favorably with that expected at magmatic temperatures based upon exchange experiments (e.g. 0·58 for An_{90} plagioclase to 0·76‰ for An_{50} plagioclase at 1300°C; Chiba *et al.*, 1989). The fractionation between basaltic liquid and olivine is not known directly from experiment, but a value of 0·32‰ is predicted at 1300°C based upon the combination of experimentally determined melt–CO_2, forsterite–calcite, and calcite–CO_2 fractionations (Muehlenbachs & Kushiro, 1974; Chiba *et al.*, 1989; Rosenbaum, 1994). However, the accumulated error in such an estimate is relatively large (∼ ±0·2–0·3‰, 1σ), so the close correspondence between this predicted value and our measured value may not be significant. An empirical model for oxygen isotope partitioning between minerals and melts (Matthews *et al.*, 1998) predicts a value of 0·4–0·5‰ for $\Delta_{melt-olivine}$ for the lava compositions considered in this study. Our results compare favorably with the range of values expected from these two independent estimates.

The fractionations of oxygen isotopes we observe among coexisting phases are within the ranges of but more restricted than fractionations observed in previous studies of phenocrysts and glass or groundmass in basic lavas (Fig. 2). Values of $\Delta_{glass-olivine}$, $\Delta_{groundmass-olivine}$, or $\Delta_{whole\ rock-olivine}$ from previous studies range from 0·2 to 2·0, and values for equilibrium melt–olivine fractionation have been suggested to be as high as 0·9–1·0‰ (Onuma *et al.*, 1970; Clayton *et al.*, 1971, 1972; Hoernes & Friedrichsen, 1977; Kyser *et al.*, 1981, 1982; Macpherson & Mattey, 1997). Our results indicate a value of ∼0·4 ± 0·1‰, significantly lower than the upper end of the range of previous data. Previous measurements of $\Delta_{plagioclase-olivine}$ are similarly more widely distributed (0·4–1·3‰) and on average larger than observed in this study (Onuma *et al.*, 1970; Clayton *et al.*, 1972; Hoernes & Friedrichsen, 1977; Kyser *et al.*, 1981, 1982). These differences may be due to the fact that ours is the first study to make a significant number of determinations of $\Delta_{glass-olivine}$ and $\Delta_{plagioclase-olivine}$

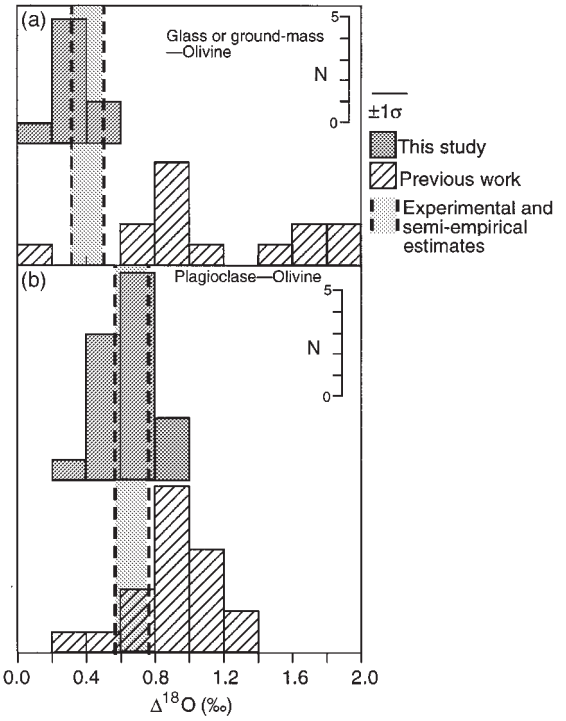

Fig. 2. Histograms illustrating the variability in $\Delta_{glass-olivine}$ (a) and $\Delta_{plagioclase-olivine}$ (b) measured in this study (dark gray boxes) and from previous studies (diagonally ruled boxes; data from Onuma *et al.*, 1970; Clayton *et al.*, 1971, 1972; Kyser *et al.*, 1981, 1982; Macpherson & Mattey, 1997). Vertical dashed lines and light gray fields illustrate the range of fractionations between olivine and either An_{50-90} plagioclase or basaltic melt at 1300°C based on experimental studies of isotope partitioning and models of isotope partitioning among silicate phases (Muehlenbachs & Kushiro, 1974; Chiba *et al.*, 1989; Rosenbaum, 1994; Matthews *et al.*, 1998).

using laser-based measurements, and therefore we may have been more successful at avoiding sample alteration and the well-known analytical difficulties associated with conventional oxygen isotope measurements of olivine (Mattey *et al.*, 1994).

Comparison with previous work

The range of $\delta^{18}O$ values we find for olivine phenocrysts (0·98‰) is a factor of 10 lower than that reported previously based on conventional fluorination measurements of whole-rock samples from oceanic arcs [summarized by Harmon & Hoefs (1995)]. Some of this difference could reflect our emphasis on olivine-bearing samples, which are primitive relative to the full range of arc-related lavas represented in the conventional data base. However, this is not likely to be the principal cause because much of the reported range in whole-rock measurements can be found in basalts, basaltic andesites, and andesites in the same arcs we have studied (Pineau *et al.*, 1976; Ito & Stern, 1985; Woodhead *et al.*, 1987; Harmon & Hoefs, 1995). We infer, as has previously been concluded from study of mantle peridotites and ocean-island basalts (Mattey *et al.*, 1994; Eiler *et al.*, 1995, 1996), that the oxygen isotope variations in olivine phenocrysts are more restricted than in whole rocks primarily because analysis of fresh phenocrysts (particularly olivines) avoids or minimizes the effects of low-temperature alteration; nevertheless, an additional factor may be that the increases in $\delta^{18}O$ that are known to build up in residual liquids from fractional crystallization (Matsuhisa *et al.*, 1973) are minimized by focusing on relatively primitive, olivine-bearing samples.

Our data contradict a conclusion reached by some previous studies of oxygen isotope variations in oceanic-arc basalts that the average value of $\delta^{18}O$ in oceanic-arc magmas, even after correction for low-temperature alteration and magmatic fractionations, is ~0·5‰ higher than for MORB and back-arc-basin basalts (Woodhead *et al.*, 1987; Harmon & Hoefs, 1995) and that this difference reflects a common and relatively large amount of subducted crustal oxygen in the sources of these arc magmas. In contrast, we find that elevations in $\delta^{18}O$ of ~0·5‰ with respect to MORB are an extreme found only in a minority of arc samples and that the sources of both arc and back-arc lavas are on average closely similar to estimates for the typical upper mantle based on measurements on MORBs and peridotite xenoliths (Fig. 1). We note that in this respect our results confirm the work of Ito & Stern (1985), who found that glasses from both the Mariana arc and trough are similar in $\delta^{18}O$ to MORB. Similarly, recent results for glasses from the Lau basin (Macpherson & Mattey, 1997) span a small range in $\delta^{18}O$ near the average value for MORB and display correlations with chemistry that are analogous to correlations displayed by our data (discussed below). Recent study of lavas from the Lesser Antilles and the Kermadec–Hikurangi margin have found larger ranges and higher average values of $\delta^{18}O$ than both MORB and the results of this study, but in both cases these differences were interpreted to reflect assimilation of continental material (Smith *et al.*, 1996; Thirlwall *et al.*, 1996; Macpherson *et al.*, 1998); these studies confirm the conclusions of Harmon *et al.* (1981), Hildreth & Moorbath (1988), and Davidson & Harmon (1989) that variations in $\delta^{18}O$ of arc-related lavas erupted through thick sequences of continental rocks or sediments dominantly reflect assimilation–fractional crystallization processes.

Correlations between $\delta^{18}O$ and sample chemistry

When comparing our oxygen isotope data with other chemical indices, it is useful to focus on a single phase to remove the effects of oxygen isotope fractionations

among different crystalline phases and glass. We have selected olivine for this purpose because it was measured in most of our samples and, for the reasons discussed above, we believe it to be a reliable monitor of $\delta^{18}O$ in unaltered and relatively primitive basaltic lavas. For the five out of 72 samples in which olivine was not analyzed, we calculated an 'equivalent olivine' value equal to the value measured in plagioclase or glass in that sample minus the average fractionation between olivine and plagioclase or glass observed in this study. Although these fractionations are well defined by our data, this correction introduces additional uncertainty for these samples; they are distinguished from the other data by parentheses in Table 1. None of the oxygen isotope variations or correlations observed in this study are significantly dependent on these five values, but they are provided for completeness. We emphasize at the outset of this discussion that all values of $\delta^{18}O$ in excess of 5·4‰ occur in lavas from the Vanuatu and New Caledonia arcs or the TLTF islands (i.e. Papua New Guinea), and we reiterate that such ^{18}O-enriched samples are atypical ($\sim$20% of our survey sampling); thus, the observed trends and our interpretations of them are biased toward processes relevant to these samples. However, the other studied suites are consistent with the trends defined by these extreme samples and therefore are consistent with the interpretation that such suites were influenced, though not as strongly, by similar processes.

Values of $\delta^{18}O$ in olivine phenocrysts in our samples are not correlated with the whole-rock SiO_2 or MgO contents of the host lavas when the data set is viewed as a whole (Table 1). We infer that the effects on $\delta^{18}O$ of magmatic fractionation and accumulation leading to such correlations for whole-rock data from arc settings (Matsuhisa *et al.*, 1973; Woodhead *et al.*, 1987) have been minimized by our emphasis on relatively primitive olivine-bearing lavas.

A key question is whether $\delta^{18}O$ values for our samples correlate with conventional chemical and isotopic monitors of slab components in the sources of arc-related lavas. To answer this question, our results for the oxygen isotope composition of olivine in arc-related lavas are compared in Fig. 3 with $^{87}Sr/^{86}Sr$ and various trace- and minor-element indices that plausibly monitor the contribution of subducted materials to the sources of arc lavas.

Values of $\delta^{18}O$ in olivine span a restricted range near the average upper-mantle value in lavas with low-$^{87}Sr/^{86}Sr$ ratios; elevated $\delta^{18}O$ values are restricted to samples at the high end of the distribution of $^{87}Sr/^{86}Sr$ (Fig. 3a). Radiogenic strontium in arc-related lavas is generally interpreted as a monitor of slab-derived contributions to their sources (Gill, 1981), and thus the relationship shown in Fig. 3a suggests that the elevated oxygen isotope ratios we observe are related to slab-derived components. The observed relationship between $\delta^{18}O$ and $^{87}Sr/^{86}Sr$ is consistent with a hyperbola that results from mixing between an Sr-poor, low-$\delta^{18}O$, low-$^{87}Sr/^{86}Sr$ component (i.e. the approximately MORB-like mantle wedge) and an Sr-rich, high-$\delta^{18}O$, high-$^{87}Sr/^{86}Sr$ component (i.e. slab-derived fluid and/or melt). It should be noted that the overall hyperbolic trend shown in Fig. 3a, although defined by the data set as a whole, is best defined by the single suite of island-arc basalts from the western Vanuatu arc (filled circles); this suite is the only group of related samples considered in this study that covers a sufficient range in $\delta^{18}O$ and $^{87}Sr/^{86}Sr$ to display the full trend. It should be noted also that correlations between $\delta^{18}O$ and $^{87}Sr/^{86}Sr$ as a result of assimilation of pre-existing crust are generally linear rather than hyperbolic, because of the similarity in Sr concentrations of arc-related lavas and older rocks in the arc crust (e.g. Davidson & Harmon, 1989); therefore, the hyperbolic relationship in Fig. 3a suggests processes other than crustal assimilation.

Arc-related lavas are characterized by distinctive enrichments and depletions in certain trace elements relative to MORB and OIB that are associated with (or defined as characteristics of) slab-derived components (Gill, 1981). Certain chemical characteristics are common to nearly all arc-related lavas and are rare elsewhere [e.g. enrichment of large ion lithophile elements (LILE) such as K, Ba, and Sr with respect to high field strength elements (HFSE) such as Ti and Nb], whereas others are thought to be diagnostic of the presence in the sub-arc mantle of distinctive components such as melts or aqueous fluids that may sample a specific part of the subducting slab (e.g. the basaltic crust vs the overlying sediments; Kay, 1980; Ellam & Hawkesworth, 1988; Elliott *et al.*, 1997; Turner *et al.*, 1997) or pre-existing 'OIB-like' enrichments in the mantle (Lin *et al.*, 1989). The number and identity of such components differ according to the set of elements considered; for example, the classification of Hawkesworth *et al.* (1997) would define all lavas considered in this study as falling within the compositional field (Sr/Th >200; Th <5 ppm) interpreted to reflect dominantly addition of a slab-derived aqueous fluid; in contrast, Elliot *et al.* (1997) concluded that sediment-derived melt controls the budgets of many trace elements in the sources of samples we have studied from the Marianas. However, certain common themes have emerged in recent studies: uranium excesses (i.e. $[^{238}U/^{230}Th] > 1$) and enrichments of fluid-soluble elements (Ba, Sr, U) with respect to non-fluid-soluble but incompatible elements (Th, Nb, Zr) are generally identified with slab-derived aqueous fluids dominated by contributions from the basaltic portions of the subducted oceanic crust (Ellam & Hawkesworth, 1988; Elliott *et al.*, 1997; Turner *et al.*, 1997); in contrast, high concentrations of Th, elevated ratios of Th and rare earth elements (REE) to Nb, strong light rare earth element (LREE) enrichments, negative Ce anomalies,

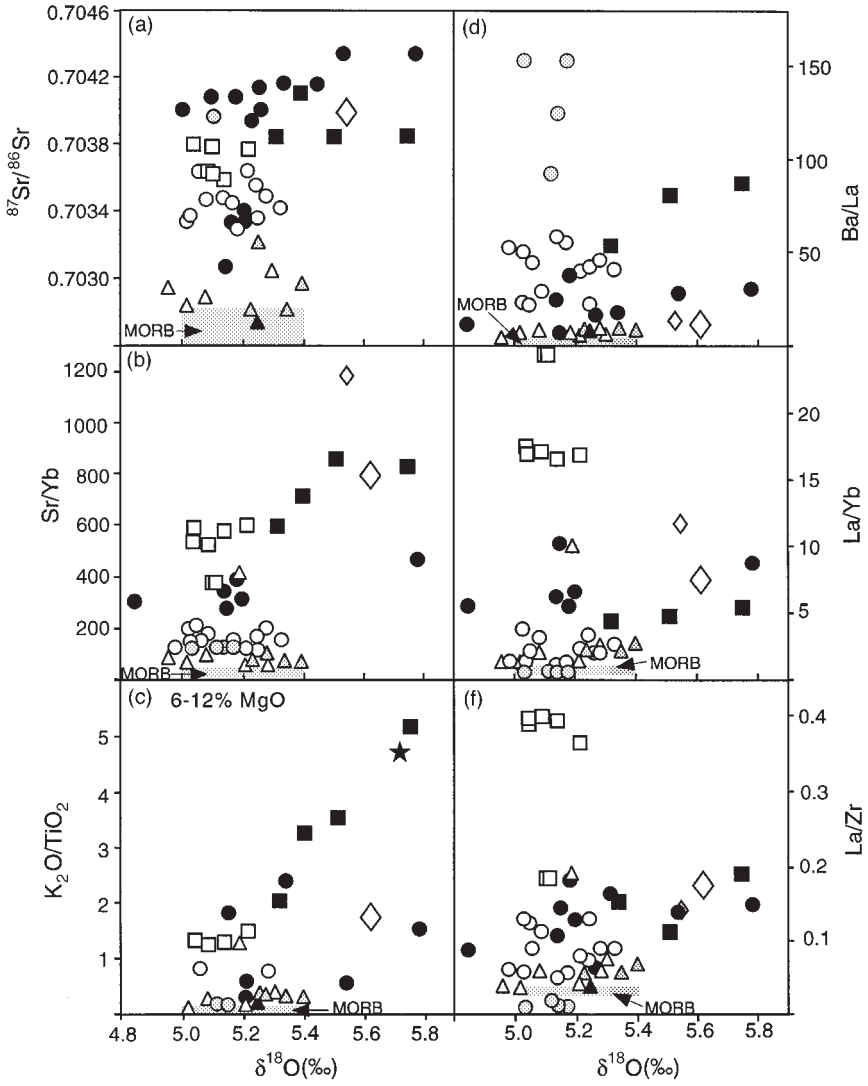

Fig. 3. Comparison of oxygen isotope ratios in olivine phenocrysts from arc and back-arc lavas with other geochemical indicators in the host lavas: (a) $^{87}Sr/^{86}Sr$; (b–f) various minor and trace element abundance ratios (by weight). Sr isotope and element-abundance ratios are either measured on the same samples (small symbols) or estimated based on data for closely related samples (large symbols). (See text for sources of trace element and Sr isotope data.) Symbols are as in Fig. 1. Gray boxes mark typical NMORB compositions (Sun & Nesbitt, 1979; Ito *et al.*, 1987; Michael, 1995). It should be noted that only lavas with MgO contents between 6 and 12 wt % are plotted in (c), to minimize the effects of fractionation on the K_2O/TiO_2 ratio. This range was selected based on the observed relationship between this ratio and MgO in Vanuatu and Mariana arc lavas.

and/or U-series isotopic compositions near the equiline (i.e. $[^{238}U/^{230}Th] \sim 1{\cdot}0$) are associated with a component of sediment-derived melt (Ellam & Hawkesworth, 1988; Elliott *et al.*, 1997; Turner *et al.*, 1997), or possibly a pre-existing 'OIB-like' enrichment in the mantle (Lin *et al.*, 1989).

Elevated values of $\delta^{18}O$ (= 5·4‰) observed in this study are generally associated with elevated ratios of highly incompatible LILE to moderately incompatible trace elements not believed to be highly fluid soluble (e.g. Sr/Yb and K_2O/TiO_2; Fig. 3b and c). These trends, although somewhat scattered, are consistent with the conclusion drawn from Fig. 3a that ^{18}O enrichments in lavas are associated with distinctive, 'enriched' components in their sources. Relationships between $\delta^{18}O$ and trace-element ratios thought to discriminate among different varieties of enriched components are complex and fail to reveal a unique association between ^{18}O enrichments and any one of the several distinctive slab-derived components currently believed to contribute to the sub-arc mantle (Fig. 3d–f). For example, arc lavas with high-$\delta^{18}O$ olivines have Ba/La ratios that are high

relative to NMORB, but they span a considerable range and are not significantly elevated in Ba/La relative to the lower-$\delta^{18}O$ arc-related lavas; in particular, the most extreme elevations of Ba/La among lavas examined in this study are in samples from the South Sandwich arc, yet these have $\delta^{18}O$ values indistinguishable from average upper mantle (Fig. 3d). It should be noted that enrichment of Ba relative to other LILE such as La is one of the most widely used indicators of contributions of fluid from the basaltic portions of the subducted slab to the sub-arc mantle (e.g. Gill, 1981; McCulloch & Gamble, 1991; Hawkesworth *et al.*, 1994), so our data do not support an exclusive association of ^{18}O enrichments with such a component. Similarly, lavas from Guguan island in the Mariana arc have $\delta^{18}O$ values for olivine within the range of olivine in typical upper-mantle peridotites (Table 1), despite spanning a significant range in [$^{238}U/^{230}Th$] ratio from 1·29 to 1·56; such large U excesses are taken as evidence that fluids from the basaltic portions of the subducting slab dominate the U and Th budget of the mantle sources of Guguan lavas (Elliott *et al.*, 1997).

High-$\delta^{18}O$ lavas are generally LREE enriched relative to NMORB and to most lower-$\delta^{18}O$ arc-related lavas (Fig. 3e). However, shoshonites from the northern Mariana arc have $\delta^{18}O$ values similar to average upper mantle, yet they display extreme LREE enrichments, demonstrating that LREE and ^{18}O enrichments are not uniquely linked in arc environments. Similarly, enrichments in LREE with respect to HFSE (e.g. La/Zr; Fig. 3f) are generally positively correlated with $\delta^{18}O$ among our samples, but the Mariana shoshonites have extreme enrichments of La with respect to Zr without any elevation in $\delta^{18}O$. Enrichments of LREE relative to heavy rare earth elements (HREE) and HFSE in arc lavas have been proposed as evidence that sediment-derived melts dominate the trace-element characteristics of enriched sub-arc mantle (Brenan *et al.*, 1995; Elliot *et al.*, 1997); the results shown in Fig. 3e and f indicate that $\delta^{18}O$ elevations are generally but not universally associated with such a signature.

Figure 3d–f thus demonstrates an important result of our study: extreme 'slab-derived fluid' signatures (e.g. Ba/La and U/Th enrichment usually identified with fluids from the basaltic component of the subducting crust) and 'sediment-derived melt' and/or 'OIB-like' signatures (e.g. LREE/HREE or LREE/HFSE enrichment) can each be present in the sub-arc mantle sources of arc-related magmas without a distinctive oxygen isotope signature. Collectively, the relationships illustrated in Fig. 3 suggest that, although elevated $\delta^{18}O$ values of arc-derived magmas are associated in general terms with commonly used trace element indicators of slab-derived components in their sources (Fig. 3a–c), the abundances of such components as measured by oxygen isotopes are not related one-to-one to the proportions of distinguishable 'slab fluid' and 'sediment melt' components based on diagnostic trace element ratios (Fig. 3d–f).

Although the relationships between $\delta^{18}O$ and commonly used trace element monitors of slab-derived components are scattered, there are several well-defined relationships between the $\delta^{18}O$ values from this study and other geochemical indices, which rather than being direct monitors of slab contributions to the sources of arc lavas are useful as monitors of the extent of melting and/or prior depletion of the peridotitic sources of basaltic melts. These relationships are illustrated in Fig. 4 and described in the following paragraphs.

TiO_2 contents

Values of $\delta^{18}O$ are compared with concentrations of TiO_2 (wt %) measured in whole-rock specimens of host lavas in Fig. 4a; samples plotted in this panel are restricted to those with 6–12 wt % MgO to minimize variations related to fractional crystallization. This figure shows that the ^{18}O-enriched samples all have low TiO_2 contents, generally less than 0·8 wt %—approximately half the average concentration in NMORB (Sun & McDonough, 1989) and at the lower end of the range observed in arc lavas (Plank & Langmuir, 1988). The overall trend shows both systematically higher TiO_2 contents for back-arc magmas (triangles) than for arc magmas with comparable $\delta^{18}O$ values and a negative correlation between TiO_2 and $\delta^{18}O$ when only the arc lavas are considered. All other things (e.g. source composition, mineralogy of the residue, and extent of fractionation) being equal, lower values of TiO_2 in basalts indicate higher extents of single-stage melting and/or melting of a more depleted (i.e. previously melted) peridotite source.

Although Fig. 4a is restricted to lavas with 6–12 wt % MgO, some of the variation in TiO_2 could still reflect superposition of the effects of fractionation on source and degree-of-melting effects. We have evaluated this by calculating values of $TiO_{2(8\cdot0)}$ for suites of related samples to correct for low-pressure fractionation (Klein & Langmuir, 1987). Eleven suites of lavas were selected that were sufficiently well sampled to permit an estimation of $TiO_{2(8\cdot0)}$ values: two islands from the Mariana arc (Guguan and Agrigan), the Mariana trough as a whole, the Scotia Sea as a whole, one island from the South Sandwich arc (Zavodovski), three islands from the Vanuatu arc (Ambrym, Tanna, and Tongoa), boninites from New Caledonia and the Hunter fracture zone (Vanuatu), and one island from the 'TLTF' arc (Lihir). TiO_2 contents of individual samples from each suite and related samples from that suite not analyzed for $\delta^{18}O$ in this study were regressed with MgO content, and the TiO_2 value of the resulting line at 8·0 wt % MgO was taken as the $TiO_{2(8\cdot0)}$ value for that suite; this value applies to all members of

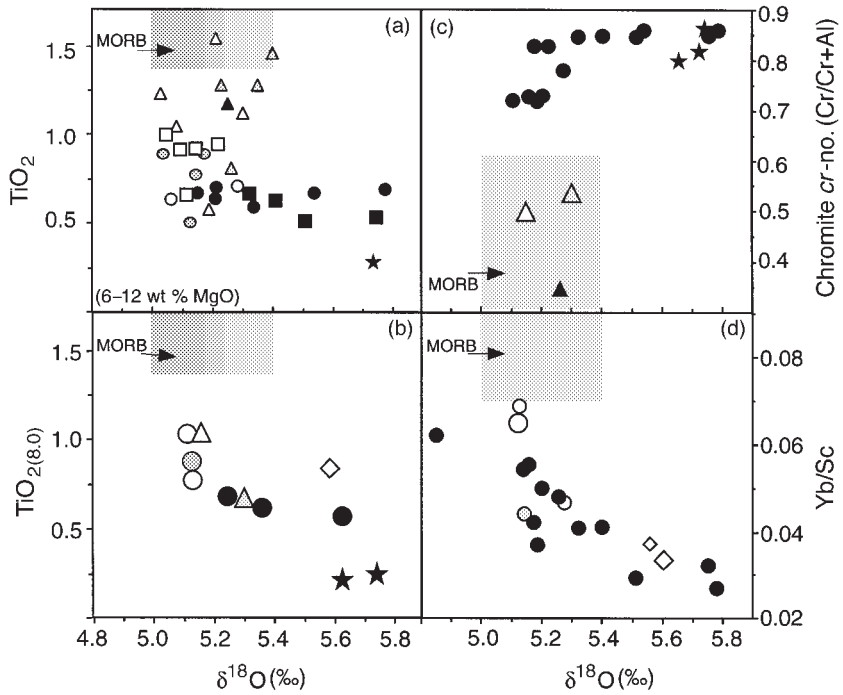

Fig. 4. Comparisons of oxygen isotope ratios in olivine phenocrysts from arc and back-arc lavas with other geochemical indicators: (a) wt % TiO_2 in the host lava; (b) $TiO_{2(8{\cdot}0)}$ values of the host lava [calculated following methods described by Klein & Langmuir (1987); see text for details]; (c) the *cr*-numbers of coexisting chromite phenocrysts [i.e. the Cr/(Cr + Al) ratio on a molar basis]; (d) the Yb/Sc ratio (by weight) of the host lavas. Gray boxes mark typical NMORB compositions. Chemical and mineral-composition data are either measured on the same samples (small symbols) or estimated based on data for closely related samples (large symbols). (See text for data sources.) Symbols are as in Fig. 1.

that suite and the $\delta^{18}O$ value is the average for one or more members of that suite analyzed for oxygen isotope composition in this study. Figure 4b confirms the key feature of Fig. 4a: elevated $\delta^{18}O$ values are associated with low values of $TiO_{2(8{\cdot}0)}$ in the host lavas, generating an overall negative correlation. Scatter about the trend in Fig. 4a is reduced in Fig. 4b. The trend in Fig. 4b is particularly well defined by data other than alkali basalts from Papua New Guinea (the open diamond). Alkali basalts, including those in arc settings, are systematically higher in Ti than related tholeiitic lavas (e.g. Shimizu & Arculus, 1975), so this discrepancy is not unexpected.

Macpherson & Mattey (1997) presented data for oxygen isotope variations in Lau basin back-arc lavas that show a subtle trend of increasing $\delta^{18}O$ with decreasing $Na_2O_{(8{\cdot}0)}$. The behavior of Na during partial melting of peridotite is, to first order, similar to that of Ti, and thus this observation is analogous to that described above. Lavas examined in this study and found to have relatively high values of $\delta^{18}O$ ($\delta^{18}O_{olivine}$ = 5·4‰) also generally have low concentrations of Na relative to the sample suite as a whole (2·1 vs 2·5 wt % Na_2O), although the overall correlation between $\delta^{18}O$ and Na_2O is not as well defined as those illustrated for TiO_2 in Fig. 4a and b.

Chrome number

Among samples containing chromite phenocrysts (approximately half of our samples; mostly from the Vanuatu suite), high $\delta^{18}O$ values are restricted to samples with chromites having chrome numbers (i.e. *cr*-number = Cr/[Cr + Al]) of 0·80 or greater (Fig. 4c). Such values are high compared with chromites in abyssal peridotites (0·1 < *cr*-number < 0·6) and most basaltic lavas (0·2 < *cr*-number < 0·7); comparable values are common only in alpine peridotites, boninites, high-Mg andesites, and, less commonly, oceanic plateau basalts (Dick & Bullen, 1984; Arai, 1994). Relatively high *cr*-number values in spinels from peridotites are interpreted as an indication that the rocks are residual to high integrated extents of melting (i.e. the total amount of melt extracted from the source, whether in single or multiple melting events, is high) or high extents of melt–peridotite reaction (Arai & Matsukage, 1996); this is because Cr is compatible and Al incompatible in peridotitic residues equilibrated with basaltic melts (Dick & Bullen, 1984). When found in basaltic phenocrysts, such spinels are similarly thought to reflect derivation of those lavas from sources that have undergone unusually high integrated extents of melting (Dick & Bullen, 1984; Arai, 1994). Thus, the association

of high $\delta^{18}O$ values with high *cr*-number suggests that the residues remaining in the sources of lavas with elevated $\delta^{18}O$ are highly depleted.

Yb/Sc

There is a negative correlation between $\delta^{18}O$ and Yb/Sc among samples from this study, regardless of geographic location and petrologic type (Fig. 4d). The Yb/Sc ratio of unfractionated, mantle-derived magmas is predicted to decrease continuously with increasing integrated extents of melting of peridotitic sources because Yb is somewhat more incompatible than Sc during peridotite melting (Klein & Langmuir, 1987). Clinopyroxene fractionation will lead to progressive increases in this ratio in residual liquids, but it should be insensitive to fractional crystallization of other phases and particularly during fractionation of olivine from relatively primitive magmas. Although care must be taken to exclude highly fractionated magmas when examining variations in Yb/Sc, observed relationships between Sc and Yb concentrations and other indices of extent of melting in both MORB and arc-related magmas (Klein & Langmuir, 1987; Plank & Langmuir, 1993) confirm that they can be a valuable measure of integrated degree of melting. We have examined the Yb/Sc relationship shown in Fig. 4d for the effects of clinopyroxene fractionation; although this process probably influenced the two highest Yb/Sc ratios, the trend is unchanged if only samples with $\geq 8\%$ MgO and/or ≥ 25 ppm Sc are plotted (a compositional range over which the effects of clinopyroxene fractionation are not expected to be significant). The correlation in Fig. 4d is therefore consistent with the relationships exhibited in Fig. 4a–c; that is, higher $\delta^{18}O$ is associated with higher extents of single-stage melting and/or higher degrees of depletion of the peridotitic sources of arc-related basalts as a result of previous melting events.

DISCUSSION

Key results of this study are that variations in $\delta^{18}O$ among arc-related lavas, although unusual, are associated with known trace element and radiogenic isotopic tracers of slab input to their sources and, more importantly, they are correlated with chemical indices that are sensitive to the integrated extent of melting of those sources. In the following discussion we develop a model for the petrogenesis of arc-related lavas that both explains this observation and is consistent with the other known characteristics of these lavas. Much of this discussion is biased toward explanation of the relationship between $\delta^{18}O$ and other characteristics of lavas from the Vanuatu–Fiji–New Caledonia region because this is the suite of samples covering the full range of $\delta^{18}O$ observed in this study. However, the samples from the other suites fall on the same overall trends, suggesting that the model we develop could apply more broadly; more work will be needed to define whether these other suites (as well as suites not considered in this study) can be understood in the framework of the same model.

Oxygen isotope shifts associated with melting and magmatic evolution

Fractionations of oxygen isotopes among coexisting minerals and melts are small at the temperatures of peridotite melting and basaltic volcanism (Chiba *et al.*, 1989; Palin *et al.*, 1996; Fig. 2), but it is possible that even small fractionations could produce the $\sim 1‰$ variations in $\delta^{18}O$ observed for olivine in this study by Rayleigh fractionation during melting or crystallization. This possibility can be tested using experimentally known and empirically estimated high-temperature fractionations of oxygen isotopes among minerals and melts.

Crystallization of olivine $\pm$ pyroxene will raise both the $\delta^{18}O$ values (Chiba *et al.*, 1989; Matthews *et al.*, 1998; Fig. 2) and TiO_2 contents of residual liquids, and therefore should produce trends opposite to that observed in Fig. 4a. Moreover, the correction of TiO_2 contents to a common MgO content should minimize the effects of fractional crystallization, and thus the variations in $TiO_{2(8{\cdot}0)}$ and the correlation with $\delta^{18}O$ shown in Fig. 4b would be difficult to account for by this process. Crystallization of Cr-rich spinel as part of a fractionating assemblage is expected to lead to progressive decreases in the *cr*-number of spinel phenocrysts in most circumstances (Arai, 1994); therefore, fractional crystallization can produce negative correlations between $\delta^{18}O$ and the *cr*-number of spinels but not trends with positive slope such as that shown in Fig. 4c for arc-related lavas. Fractionation of clinopyroxene rapidly removes Sc from magmas, such that Yb/Sc ratios in low-MgO lavas can be high (>0·1, based on data reported in the references in the 'Samples and analytical methods' section for evolved lavas in the arcs we have studied). However, the MgO and Sc concentrations of the samples defining the trend in Fig. 4d (average 8 wt % and 35 ppm) are substantially higher than those typical of such fractionated magmas (<5 wt % and <25 ppm). In any case, fractionation of clinopyroxene is expected to produce a positive trend in Fig. 4d rather than the negative one that is observed (i.e. because it raises both the $\delta^{18}O$ and Yb/Sc of residual magma). The relationships observed in Fig. 4 are therefore at odds with the expected effects of fractional crystallization, and we conclude that such processes are not major factors in the observed covariations between $\delta^{18}O$ and other geochemical and petrological indicators.

The difference in $\delta^{18}O$ between basaltic melt and a residual peridotitic mineral assemblage during mantle

melting is expected to be a small positive number (~0·2‰; Chiba *et al.*, 1989; Matthews *et al.*, 1998; Fig. 2), and thus even extensive fractional melting of peridotite will produce depleted residues that are only slightly lower in $\delta^{18}O$ than initial fertile sources (e.g. 20% fractional melting lowers $\delta^{18}O$ of the residue by only 0·04‰). This expectation is confirmed by analysis of olivine and pyroxene from highly depleted harzburgites of the Voykar massif, Polar Urals: these rocks are thought to be residual to 15% fractional melting (Sharma *et al.*, 1997), yet they contain olivines that are indistinguishable in $\delta^{18}O$ from those in average fertile mantle peridotite (Eiler *et al.*, 1996). Based on this and the predicted effects of melting on elemental abundances described above (i.e. residues will have lower TiO_2 and Yb/Sc, and their spinels will have higher *cr*-number), melting alone could therefore only produce correlations in Fig. 4 that are opposite in slope from those observed (and in any case so steep so as to appear vertical at the scale plotted). We therefore conclude that equilibrium partitioning of oxygen isotopes during simple batch or fractional fusion of peridotite cannot produce the trends in Fig. 4.

Given that fractionation of oxygen isotopes during melting or crystallization cannot explain the observed relationships between oxygen isotopes and sample chemistry, variations in $\delta^{18}O$ observed in this study are most simply interpreted in terms of mixing of two or more isotopically distinct reservoirs. High-level assimilation of oceanic crust and/or the island-arc volcanic edifice has been suggested as a way to introduce ^{18}O-enriched material into mantle-derived magmas (Harmon *et al.*, 1981; Hildreth & Moorbath, 1988; Davidson & Harmon, 1989). Although the effects of assimilation are widespread in arc-related environments, particularly in evolved magmas from arcs with thick crustal sections of continental rocks or sediments, it is difficult to explain by such a mechanism the relationships between $\delta^{18}O$ and sample chemistry observed in this study. In particular, this explanation would require preferential addition of crustal assimilants to lavas that are relatively high-degree mantle melts and/or are derived from relatively depleted mantle sources; moreover, such a process is not expected to generate the relationship between $\delta^{18}O$ and $^{87}Sr/^{86}Sr$ shown in Fig. 3a (i.e. assimilation of crustal rocks generally leads to more linear trends in these dimensions; Davidson & Harmon, 1989); finally, assimilation–fractional crystallization (AFC) processes generally produce the largest deviations in $\delta^{18}O$ in the most fractionated samples (DePaolo, 1981; Taylor, 1986) and therefore would produce trends generally opposite those observed in Fig. 4 (for reasons similar to those discussed above in reference to fractional crystallization). We conclude that although it would be possible to construct models of assimilation processes consistent with the trends in Figs 3 and 4, such models would contrast with the typical behavior of systems influenced by AFC processes.

Fluxed melting—a model for the interactions between slab-derived fluid or melt and the sub-arc mantle

A possible explanation for the correlations in Figs 3 and 4 is that peridotites in the sub-arc mantle span a restricted range in $\delta^{18}O$ (~5·0–5·2‰ for olivine; 5·3–5·5‰ for the bulk peridotite), comparable with the average value of $\delta^{18}O$ elsewhere in the upper mantle (Ito *et al.*, 1987; Mattey *et al.*, 1994; Eiler *et al.*, 1996), and that addition of a high-$\delta^{18}O$, slab-derived component is closely linked to enhanced melting of these sources. This explanation is attractive for several reasons:

(1) as described in the Introduction, 'slab' signatures in the geochemistry of arc-related lavas are plausibly attributed to the transfer of aqueous fluids and/or hydrous silicate melts from the slab to the mantle wedge. Both of these metasomatic agents would probably be derived from sediments and/or hydrated basalts in the upper portions of the subducted crust because these regions either have high initial water contents or become water rich through low-temperature sea-floor alteration; as there are several high-$\delta^{18}O$ components in the top half of the subducted crust, it is thus further expected that addition of either of these slab-derived metasomatic agents to mantle peridotite will raise its $\delta^{18}O$.

(2) Addition of water-rich components (whether aqueous fluids or hydrous silicate melts) decreases significantly the solidus temperature of peridotite at the pressures and temperatures of the sub-arc mantle (Kushiro *et al.*, 1968; Hirose & Kawamoto, 1995; Gaetani & Grove, 1998), and thus metasomatism and ^{18}O enrichment are expected *a priori* to be accompanied by enhanced melting of the mantle wedge.

(3) An additional feature of this explanation is that it relates variations in $\delta^{18}O$ and chemical composition among our studied samples by a relatively simple common mechanism, and it is therefore suitable for examination with a detailed forward model. In this section we develop such a model to elaborate and test this hypothesis. The model is constructed with specific reference to variations in $\delta^{18}O$, chemical composition, and Sr isotope ratio among lavas from the Vanuatu–Fiji–New Caledonia region, but we also examine its consistency with the presence or absence of high $\delta^{18}O$ lavas in other suites.

Before detailing this model, we note a possible alternative is that the sources of arc lavas are variably depleted before addition of a volatile-rich slab component and that the extent to which such a component is added is a function of the extent of prior depletion. This model reverses the causality of the model detailed in this

discussion by requiring that the extent of depletion in the sub-arc mantle has some means of limiting or controlling the amount of slab-derived component that can be added to it. This might be possible if, for example, the permeability of depleted peridotite with respect to flow of slab-derived fluids or melts were higher than that of fertile sources (Toramaru & Fujii, 1984) or due to differences in the melt productivity of depleted vs fertile peridotites having equal abundances of slab-derived components. We have not developed a forward model for this hypothesis, but improved understanding of these phenomena may permit detailed examination of such models in the future.

General features of the model

Our model of the mantle sources of arc lavas relates quantitatively the abundance of slab-derived constituents in these sources to oxygen isotope ratios and other geochemical signatures of arc lavas and to the productivity of melting in the mantle wedge. We accomplish this by integrating what is known of the productivity of isobaric, isothermal, wet peridotite melting (Hirose & Kawamoto, 1995; Gaetani & Grove, 1998; Hirschmann *et al.*, 1999), trace element partitioning between basaltic melts and residual peridotitic assemblages (see the Appendix), and approximations of the geochemical properties of slab-derived fluids and melts. We acknowledge at the outset that we have made a number of simplifying assumptions that must be elaborated upon and/or modified if this geochemical and petrological model is to be explicitly integrated with dynamical models of subduction zone processes.

We assume that pre-metasomatic sources in the mantle wedge consist of peridotite having concentrations of most major and minor elements based on the 'mm3' synthetic peridotitic mix of Baker & Stolper (1995), but with approximately half the Cr_2O_3 and somewhat less Al_2O_3 to be comparable with other estimates of the composition of relatively fertile upper-mantle peridotite. We also assume that these sources have abundances of selected minor and trace elements that will, on 5% batch melting (using partition coefficients detailed in the Appendix), produce a melt with a composition near the low-$\delta^{18}O$ ends of the data arrays in Figs 3 and 4. This composition is listed in Table 2 and is broadly similar to (but somewhat more depleted than) the inferred sources of NMORB (Sun & McDonough, 1989; McKenzie & O'Nions, 1995; Hirschmann & Stolper, 1996). The initial value of $\delta^{18}O$ for olivine in this source is assumed to be 5·0‰ (approximately the low-$\delta^{18}O$ end member to trends in Figs 3 and 4), implying a whole-rock value of ~5·3‰ (Chiba *et al.*, 1989; Mattey *et al.*, 1994).

The source is assumed to be held at a constant temperature and pressure (detailed below) while either a high-$\delta^{18}O$ aqueous fluid or a water-rich silicate melt is added to it. We first describe the assumed composition of the model aqueous fluid; we estimate below the composition of the model hydrous silicate melt. The fluid is

Table 2: Composition of components for fluxed melting models

	Fertile peridotite	Slab melt	Slab fluid*
wt %			
SiO_2	45·4	57·82	6·00
TiO_2	0·17	0·72	0·00
Al_2O_3	3·57	17·35	1·00
Cr_2O_3	0·31	0·00	0·00
FeO†	7·11	4·53	0·00
Mn	0·13	0·00	0·00
MgO	38·2	1·71	0·00
NiO	0·23	0·00	0·00
CaO	3·57	2·31	0·00
Na_2O	0·31	1·85	2·00
K_2O	0·03	3·70	1‡/11§
H_2O	0·00	10·00	90·00
ppm			
Rb	0·028		224
Ba	0·317		2373
Sr	5·87		4572
La	0·138		61
Ce	0·44		123
Nd	0·472		72
Sm	0·197		18
Eu	0·081		6
Gd	0·319		*18·8*
Dy	0·414		*15·5*
Ho	0·099		2·6
Er	0·305		*5·9*
Yb	0·48	1	0*/2·7**
Lu	0·057		1·1
Y	2·71		100
Th	0·011		11·2
U	0·0042		4·7
Zr	5·451		401
Nb	0·137		10

*Trace element composition is average of fluxed fractional melting models (Fig. 7b). Italicized values are derived by interpolation between MORB-normalized concentrations for adjacent rare earths.
†FeO indicates total iron as FeO.
‡Initially assumed.
§Solved for in the section 'Slab melt or slab fluid?' of the Discussion.

assumed to be 90 wt % H_2O, 6 wt % SiO_2, 2 wt % Na_2O, 1 wt % K_2O and 1 wt % Al_2O_3, and to contain no Ti, Cr, Yb, or Sc. This composition is based upon the solubility of major elements in water in equilibrium with silicate minerals at 15–20 kbar and 600–1100°C (Schneider & Eggler, 1986), plausible concentrations of Ti, Yb, and Sc in upper-crustal sediments and rocks in the slab (Albarède & Michard, 1989; Plank & Langmuir, 1998), the results of trace-element partitioning experiments between aqueous solutions and silicate minerals (Brenan *et al.*, 1995; Keppler, 1996), and the assumption that Cr has a low concentration in the fluid phase. The abundances of other minor and trace elements in this model fluid will be considered in more detail in the section on concentration of solutes, but we note here that we do not assume that the composition of this fluid corresponds in these respects to any of the several previously proposed compositions of slab-derived components [e.g. the 'slab fluid' vs 'slab melt' of Elliott *et al.* (1997)].

We assume a $\delta^{18}O$ value of 20‰ for our model fluid, intermediate between observed values in siliceous glasses from arc xenoliths (Eiler *et al.*, 1998; P. Schiano & J. M. Eiler, unpublished data, 1999) and the highest values expected in subducted sediments and volcanoclastic rocks in the upper kilometer of the subducted crust (Kolodny & Epstein, 1976; Arthur *et al.*, 1983; Muehlenbachs, 1986; Plank & Langmuir, 1998). Oxygen isotope fractionation between water and silicate and carbonate minerals at temperatures higher than 500°C is negligible (2‰; O'Neil & Taylor, 1967) and has not been considered in our estimate. If a slab-derived fluid or melt moved through the mantle wedge by percolation such that it exchanged efficiently with surrounding peridotite, its oxygen isotope composition would come into equilibrium with the peridotite through reaction, solution–reprecipitation, and diffusive exchange. Therefore, implicit in our model is the assumption that slab-derived components can be introduced into the melting region without having fully exchanged with a 'chromatographic column' of normal mantle. Movement of fluids or melts by fracture propagation or through veins is a plausible physical mechanism for satisfying this condition.

A parallel set of calculations was made assuming that the fluxing agent is a water-rich silicate melt with the same $\delta^{18}O$ value (20‰) as the model aqueous fluid described above. The model melt composition is given in Table 2 and is based on experimental melts of red clay at 15–20 kbar and 900–950°C (Nichols *et al.*, 1994; Johnson & Plank, 1999). We assumed that the model silicate melt contains 1 ppm Yb and 30 ppm Sc based on measurements of hydrous, siliceous glasses in mantle xenoliths from above subduction zones (Schiano *et al.*, 1995).

Description of wet melting

If the starting peridotite composition is held at a temperature and pressure between its dry and wet solidi and outside the stability limits of hydrous minerals in a peridotitic assemblage, addition of the aqueous fluid or hydrous melt will flux melting. Under these conditions, the increment in the melt fraction (∂F) per increment of the mass fraction of fluid in the source ($+\delta X_{fl}$; note that both F and X_{fl} are fractions relative to the total mass of the system, which changes with addition of fluid or melt) is a function of pressure, temperature, and the compositions of the fluid and peridotite. We used the MELTS algorithm (Ghiorso *et al.*, 1994) to estimate $\partial F/\partial X_{fl}$ (which we refer to as the 'productivity' for isobaric, isothermal, fluid-enhanced melting) for addition of the assumed aqueous fluid or hydrous melt to the model peridotite source. Using this algorithm, the fluid or melt phase was added to the initial solid source in increments of 0·1 wt % at a pressure of 10 kbar and a temperature of 1200°C; these conditions were chosen to be within the pressure range at which MELTS accurately describes the equation of state of water ($\leq$10 kbar; Hirschmann *et al.*, 1999) and $\sim$50°C below the MELTS-calculated dry solidus of the model peridotite at that pressure. We assume that the calculated productivity of wet melting under these conditions approximates the productivity under similar conditions at the higher pressures at which melting in the mantle wedge is believed to take place (e.g. at 20 kbar and $\sim$1300°C or 30 kbar and $\sim$1400°C; Plank & Langmuir, 1988). A calculation of this type at the more relevant, higher pressure conditions is precluded by the absence of data on the productivity of hydrous melting and the inaccuracy of the model for water used by MELTS under these conditions. In our view, a 'homologous' calculation at lower pressure of the sort we have performed is at this time the best and most quantitative compromise for modeling these processes.

MELTS calculations of productivity were made for two types of models of melt generation: (1) nearly fractional melting (i.e. extraction of each increment of melt generated after addition of each increment of 0·1 wt % fluid; bold curves in Fig. 5), and (2) batch fusion (i.e. the melt generated after each increment of fluid added to the source remains in the source in equilibrium with the residue; fine curves in Fig. 5). Calculations for three fluxing agents are shown in Fig. 5: results for addition of model aqueous fluid described above are shown as continous black curves; results for fluxing with the model silicate melt described above are shown as dashed black curves; and results for addition of pure water are shown as continuous gray curves for comparison with more compositionally complex fluxing agents. Figure 5a shows the melt fraction as a function of the amount of flux added to the source; Fig. 5b shows the melt fraction as

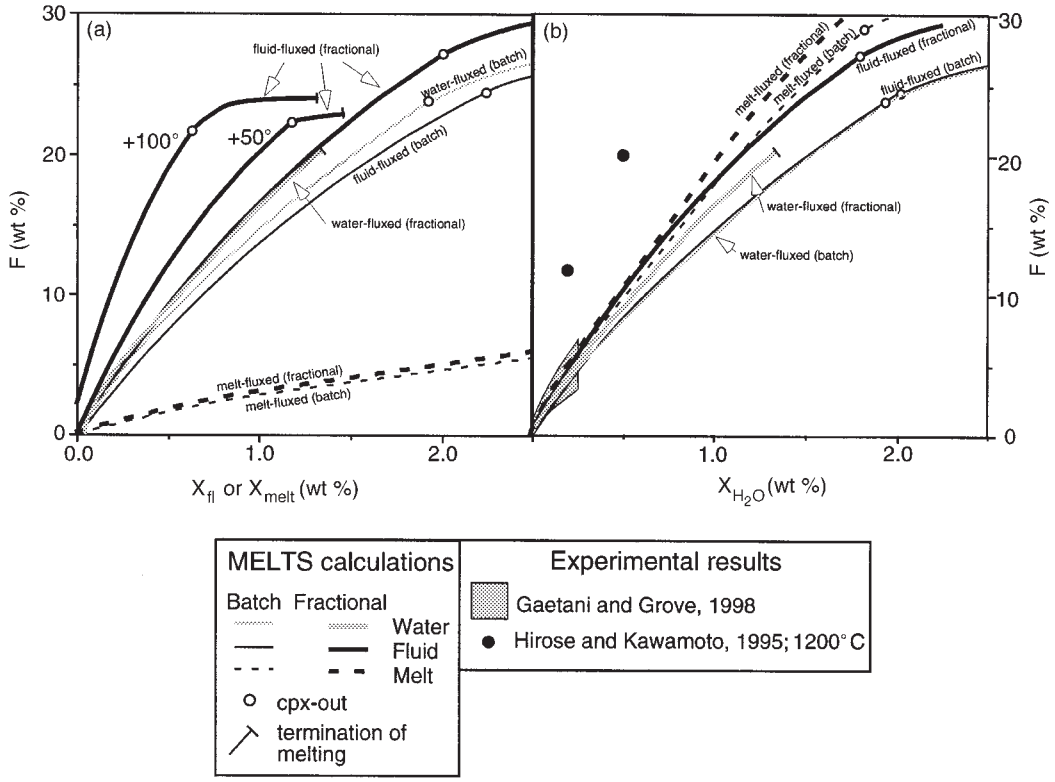

Fig. 5. (a) MELTS-calculated relationships between the extent of melting (F, in wt %) of model peridotite (Table 2) and the amount of a slab-derived water-rich phase (X_{fl}, in wt %) added to that peridotite at a temperature of 1200°C (unless otherwise marked) and a pressure of 10 kbar. The temperature was chosen to be ~50°C below the MELTS-calculated dry solidus for the peridotite composition at 10 kbar. The continuous black curves are for addition of a solute-rich aqueous fluid (Table 2); the dashed black curves are for addition of hydrous silicate melt (Table 2); and the continuous gray curves are for addition of pure water. Bold curves are for nearly fractional melting (i.e. removal of melt from the residue following addition of each small increment of slab phase); fine curves are for batch melting (retention of melt in equilibrium with the residue over full range in extent of melting). Small open circles indicate the conditions of clinopyroxene exhaustion from the residue. Truncation of a curve with a short perpendicular line indicates that further addition of fluid or melt does not drive further melting under the conditions of the calculation (i.e. because the wet solidus is higher than the assumed temperature). Heavy black curves marked '+50°C' and '+100°C' indicate models of fractional melting fluxed with model aqueous fluid at higher temperatures than assumed for all other calculations. The '+50°C' calculation is approximately at the dry solidus of the initial peridotite; in the case of the '+100°C' calculation, an increment of 5% batch melting takes place before addition of any fluid or hydrous melt. (b) reproduces the results in (a) but uses the water content of the system as the abscissa, illustrating that components of the fluxing agent other than water have little effect on the productivity of fluxed melting. The shaded field in (b) spans a range of estimated curves independently calculated based on hydrous melting experiments (Gaetani & Grove, 1998); filled circles in (b) illustrate results for wet batch melting experiments near the dry peridotite solidus (Hirose & Kawamoto, 1995), and are expected to be comparable with our '+50°C' curves.

a function of the amount of water added to the source by the fluxing agent.

The models of productivity for both fractional and batch fusion fluxed by the model aqueous fluid yield a similar result: $\partial F/\partial X_{fl}$ decreases steadily from ~20 wt % melt per wt % fluid in the mixed source at the first introduction of fluid, to 15 wt % melt per wt % fluid at 15% melting and 10 wt % melt per wt % fluid at 30% melting. The model results for addition of pure water and the more complex aqueous fluid are not significantly different; this is well illustrated by the comparison in Fig. 5b, which normalizes out the difference in water content between these two fluxes (see below). Figure 5b shows that the MELTS model predicts a relationship between X_{fl} and F for pure H_2O similar to the results of Gaetani & Grove (1998) for a small range of temperatures near the dry solidus and less productive—by about a factor of two—compared with the results of Hirose & Kawamoto (1995) for melting slightly above the dry solidus (i.e. at relatively higher temperatures than assumed for most of our model calculations) fluxed by low total amounts of water; the comparison with experiments suggests that, in agreement with the analysis of Hirschmann *et al.* (1999), the MELTS algorithms provide a reasonable quantitative basis for modeling the productivity of hydrous melting. It should be noted that several previous treatments of the productivity of fluid-enhanced melting have considered the effects of flux addition well above the

temperature of the dry solidus, and therefore produced higher estimates of the productivity ($\partial F/\partial X_{fl}$) (Stolper & Newman, 1994; Hirose & Kawamoto, 1995; Gaetani & Grove, 1998; Hirschmann *et al.*, 1999). Calculated curves for fractional fusion on addition of the model aqueous fluid are shown at 50 and 100°C higher temperatures (i.e. at the dry solidus and 50°C above the dry solidus; labeled continuous lines, Fig. 5a) and to illustrate the sensitivity of productivity to temperature according to the MELTS model.

Figure 5a shows that the calculated productivity of melting fluxed by hydrous silicate melt is substantially lower on a weight-fraction basis than is that for aqueous fluid or pure water. This is a consequence of the lower concentration of water (10 wt %; Table 2) in the model silicate melt relative to the model aqueous fluid. Our calculations suggest that, regardless of the metasomatic agent, it is primarily the water content of the system that dictates the productivity of fluxed melting (although other incompatible elements have similar but less extreme effects; Kushiro, 1975; Hirschmann *et al.*, 1999). This is illustrated in Fig. 5b, in which X_{fl} (i.e. the mass fraction of the fluxing agent in the system, whether it is pure water, solute-rich aqueous fluid, or hydrous melt) has been replaced on the abscissa by X_{H_2O}, the mass fraction of water in the system. In these coordinates, melting fluxed by all the water-rich phases we have considered has a comparable productivity of ~12–16 wt % melt per wt % H_2O added to the system. This is important for understanding our efforts described in the next section in this discussion to discriminate aqueous fluid from silicate melt as the metasomatic agent that could have produced the trends in Figs 3 and 4. Figure 5 also shows that according to the MELTS calculations, variations in the composition of the metasomatic phase or the mode of melting (i.e. batch vs fractional) have only small effects on the productivity of fluxed melting and on the extent of melting at which clinopyroxene is exhausted from the residue (marked by circles in Fig. 5a and b). In addition, it should be noted that fractional melting fluxed by pure H_2O (or by aqueous fluid for the higher temperature calculations) does not proceed beyond 22–24 wt % melting under the conditions of our calculations because the temperature of the wet solidus rises to higher than the assumed temperature, reflecting the highly refractory nature of residues of pure fractional melting that have not been sufficiently refertilized by Na and Al in the fluxing agent.

Element partitioning during melting

To maintain consistency with the relationships between F and X_{fl} shown in Fig. 5, we also used MELTS to calculate the phase proportions of the residue as a function of progressive fluid- or melt-fluxed melting. Again, we carried out these calculations for batch fusion and for incremental fractional fusion. Batch and incremental fractional fusion fluxed by the model aqueous fluid or by pure H_2O yielded melting reactions up to the exhaustion of clinopyroxene (at ~25–30% melting) approximated by the reaction (given in units of mass)

$$\text{Clinopyroxene}_{9\cdot8} + \text{Oxthopyroxene}_{9\cdot9} + \text{Spinel}_{1\cdot5} + \text{Fluid}_{1\cdot0} = \text{Melt}_{14\cdot6} + \text{Olivine}_{7\cdot6}. \quad (1)$$

The melting reaction for fluxing by hydrous silicate melt differs substantially from this:

$$\text{Clinopyroxene}_{0\cdot9} + \text{Olivine}_{0\cdot2} + \text{Spinel}_{0\cdot1} + \text{Melt}^1_{1\cdot0} = \text{Melt}^2_{1\cdot7} + \text{Orthopyroxene}_{0\cdot5}. \quad (2)$$

The partitioning of minor and trace elements among coexisting phases was calculated for each melting increment using the phase proportions output by the MELTS calculations plus solid–melt partition coefficients. For each element, the partition coefficient between melt and each solid phase was taken from published experimental studies (referenced in the Appendix) and was assumed to be constant. Residue–melt partition coefficients were then calculated after each increment of melt production based on the phase proportions in the residue. The *cr*-number of chromite was described using the observed relationships among *cr*-number, F, and the Al_2O_3 content of the residue from the wet peridotite melting experiments of Hirose & Kawamoto (1995; see the Appendix). The MELTS calculations produced similar trends of *cr*-number vs F, but these results were not used because MELTS does not allow for Cr partitioning into pyroxenes.

Model algorithm

Given the assumed compositions of the metasomatizing aqueous fluid or hydrous melt and of the peridotite source (Table 2), the productivity and stoichiometry of fluxed melting output by MELTS [illustrated in Fig. 5a and approximated by the melting reactions given by equations (1) and (2)], and values for the solid–melt partition coefficients (see the Appendix), modeling of fluxed melting of the mantle wedge is straightforward. The bulk composition of the source (including its isotopic composition) is recalculated after the addition of every increment of fluid to the peridotite source. The phase proportions of this modified bulk composition are then calculated using the MELTS algorithm, and the trace elements are partitioned between the melt and solid phases according to the phase proportions and the assumed constant mineral–melt partition coefficients. Oxygen isotopes are assumed not to be fractionated between the residue and melt (i.e. we argued above that such effects are insignificant), and

the $\delta^{18}O$ of the source increases nearly linearly with X_{fl}. For the batch melting case, the calculation is made for a range of amounts of fluid added to the initial source; for the fractional fusion calculation, the bulk composition of the source at each step is taken to be that of the solid residue before the next increment of fluid is added (although F and X_{fl} are, as indicated above, normalized to the total mass of the system, including the removed melt).

Results

The results of these calculations are compared with our data in Fig. 6. In Fig. 6b, we compare the output of our model with the trend plotted in Fig. 4b rather than with that in Fig. 4a because $TiO_{2(8\cdot0)}$ is more resistant to the effects of crystallization differentiation than is raw TiO_2 content. Each figure contains fine and bold curves representing the batch and fractional melting models. Faint symbols reproduce the data from Fig. 4. Continuous curves illustrate the results of our model for addition of aqueous fluid; dashed curves are based on a model of melting fluxed by hydrous melt. It is clear that the forward models of fluxed melting driven by aqueous fluid capture the overall trends of the correlations we observed and do so simultaneously for correlations among $\delta^{18}O$, crystal chemistry (*cr*-number), major element composition ($TiO_{2(8\cdot0)}$), and trace element ratios (Yb/Sc). In contrast, models of fluxed melting driven by our model silicate melt fail to describe, or even approach, the observed trends; the possible significance of this discrepancy will be discussed in the following section.

Fractional melting calculations of fluid-fluxed melting are particularly successful at matching the data trends, whereas the batch melting calculations of fluid-fluxed melting produce less depleted lavas (i.e. higher TiO_2 and Yb/Sc) for a given amount of addition of aqueous fluid. In detail, the fractional fusion model predicts: (1) a gently curved trend of increasing $\delta^{18}O$ with decreasing $TiO_{2(8\cdot0)}$; (2) a four-fold rise in the *cr*-number of residual chromite with a relatively subtle rise in $\delta^{18}O$ (i.e. remaining within the range of 'normal' mantle peridotite), followed by a sharper rise in $\delta^{18}O$ at nearly constant *cr*-number; (3) a slightly curved, almost linear, trend of increasing $\delta^{18}O$ with decreasing Yb/Sc. The agreement between model and data is particularly good for the plot of Yb/Sc ratios vs $\delta^{18}O$ (Fig. 6c). As pointed out previously, the alkali basalts from the TLTF volcanoes fall off the trend defined by the rest of the data in Fig. 4b, and thus they also deviate from the model calculations in Fig. 6b. Given that these samples are not members of the Vanuatu–Fiji–New Caledonia suite for which our model was constructed, we do not try to explain this deviation in detail; however, as noted above, these lavas are the only alkali basalts considered in this study, and elevated TiO_2 contents are

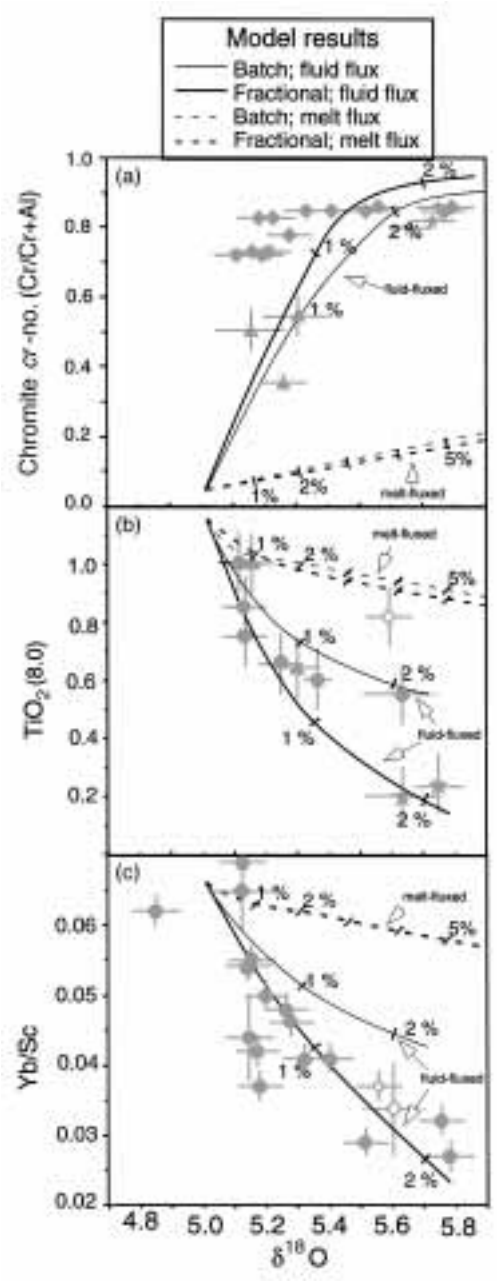

Fig. 6. Comparison of data from this study (gray symbols, reproduced from Fig. 4b–d) with calculated trends for fluxed batch fusion (fine continuous lines) and fluxed fractional fusion (bold continuous lines) models assuming an aqueous fluid as the flux; fine and bold dashed lines show the equivalent models assuming a hydrous melt as the flux. The batch and fractional models of slab-melt-fluxed melting (dashed fine and bold curves) overlap in (c). All calculations assume an initial peridotite source given in Table 2. Tick-marks indicate the total amounts of fluid or melt introduced to the source in 1% increments. (See text for further details.) It should be noted that in (a) the calculated relationship between *cr*-number and F is based on the observed relationships among *cr*-number, F, and bulk Al content in the residue during wet peridotite melting (Hirose & Kawamoto, 1995). For (b), the calculated TiO_2 contents of model melts were normalized to $TiO_{2(8\cdot0)}$ values by calculating the low-pressure differentiation of model melts using the MELTS algorithm.

a characteristic of alkalic lavas that may be due to differences in the initial fertility and/or mineralogy of the source and/or their fractionation history.

Quantitative comparison of the data with the model calculations suggests that most of the studied lavas from the Vanuatu–Fiji–New Caledonia suite could be derived from portions of the mantle fluxed by up to ~1·0 wt % of aqueous fluid from the slab, but that some lavas (boninites, low-TiO_2 shoshonites, and low-TiO_2 island-arc basalts) require fluxing of the mantle by up to ~2·5 wt % of such a fluid. Formation of the back-arc-basin basalt from the Hunter ridge (Vanuatu sample 123/3) requires fluxing by no more than ~0·25 wt % of this fluid based on the low integrated extent of melting of its source and its $\delta^{18}O$ value; however, we note that the sources of back-arc magmas could be initially less depleted than those of arc lavas, which may typically have been previously depleted by the extraction of back-arc magmas (Woodhead *et al.*, 1993; Stolper & Newman, 1994), so the two groups of magmas may not be simply related by a continuous model of the sort we have developed here. Inspection of Fig. 6 demonstrates that samples other than members of the Vanuatu–Fiji–New Caledonia suite are also consistent with our model curves and therefore could reflect similar processes. In particular, the alkaline TLTF (Papua New Guinea) suite conforms to the model trend in Fig. 6c and the less 'depleted' chemical compositions and low $\delta^{18}O$ values in Mariana and South Sandwich arc lavas are consistent with a lower abundance of a slab-derived fluxing agent in their sources than is present in higher-$\delta^{18}O$, more depleted lavas from the Vanuatu–Fiju–New Caledonia suite. More confident generalization of our model will require discovery of new suites that vary substantially in both $\delta^{18}O$ and apparent integrated extent of melting.

Slab melt or slab fluid?

Comparison of our observations with model curves for fluxing with hydrous silicate melt (dashed curves, Fig. 6) suggests that addition of a slab-derived melt to the mantle wedge cannot reproduce the trends of our observations. In particular, melt-fluxed models generate curves that, although similar in shape to those generated by fluid-fluxed models, are too shallow to explain the data. To first order, this simply reflects the facts that water is the major fluxing agent (Fig. 5b) and that the concentration of water is much higher in the aqueous fluid than in the hydrous melt. These calculated trends also reflect the high concentrations of TiO_2 and Al_2O_3 in the model silicate melt when compared with the model aqueous fluid (i.e. the model melt actually enriches the source in these elements during fluxing). An important limitation of the melt-fluxed model as we have developed it is that given the TiO_2, Al_2O_3, and Yb contents of the model silicate melt (Table 2), the low extents of melting per increment of fluxing (Fig. 5a), and the partition coefficients for these elements during peridotite melting (given in the Appendix), melting fluxed by sediment-derived melt cannot produce lavas at the extremes of the observed trends (TiO_2 <0·8 wt %; *cr*-number > ~0·3, Yb/Sc <0·05).

However, it is important to note that our model contains many variables (e.g. the composition of model hydrous silicate melt, the conditions under which it interacts with the mantle wedge, etc.), changes in which might permit fluxing of the mantle wedge by hydrous melt to produce trends such as those in Fig. 4. We have explored a number of such alternative models; although full description of these alternatives would require a digression from our discussion, the following are examples of conditions under which models similar to those described above can match our results using slab-derived melt as a fluxing agent. For example, we can match the observed trends if the metasomatizing hydrous melt is similar to model aqueous fluid in having near-zero abundances of Al, Ti, and Yb and if it has a relatively low $\delta^{18}O$ value of 10‰ (similar in $\delta^{18}O$ and Ti content to hydrous silicate glass in mantle nodules from Lihir island, but much lower in Al and Yb content than them; Eiler *et al.*, 1998). Alternatively, we can generate successful models if the slab-derived melt is water rich (30 wt % H_2O), low in $\delta^{18}O$, and intermediate between our standard model melt and the model aqueous fluid (Table 2) in Al, Ti, and Yb. Finally, successful models can result if slab-derived melt is the fluxing agent provided that it is poor in Al, Ti, and Yb and interacts with the mantle wedge at temperatures on the order of 100°C higher than the dry peridotite solidus. An important characteristic of all these successful models is that they require addition of up to 20 wt % of the metasomatizing melt to the mantle wedge to generate the observed trends; this simply reflects the need to bring in sufficient H_2O to generate the required levels of depletion in the source. Although not *a priori* unphysical, the requirement of such large amounts of slab-derived melt [almost two-thirds of the total amount of melt produced by the melting reaction; see equation (2)] appears to be a necessary feature of successful models of melt-fluxed melting and thus may lead to tests of the plausibility of this process. Overall, although we can develop successful melt-fluxed models, all require choices of slab melt properties (e.g. low Al, Ti, Yb, and $\delta^{18}O$) and/or temperatures in the mantle wedge and quantities of flux that are restrictive and not obviously compatible with experimental constraints on the compositions of slab-derived melts (Nichols *et al.*, 1994; Johnson & Plank, 1999) or with thermal models of the sub-arc mantle (Peacock, 1996). Nevertheless,

although we do not favor these versions of our model, we emphasize that neither can we rule them out.

The overall results of our modeling are that fluxing of a relatively cool mantle wedge by solute-rich aqueous fluids describes the characteristics of high-$\delta^{18}O$, arc-related lavas without the need for adjustments (i.e. beyond the assumed constraints taken from previous studies cited above and the general characteristics assumed for our model), but that the relationship between indices of extent of melting and $\delta^{18}O$ can only be described by fluxing the mantle wedge with hydrous slab-derived melts if large adjustments are made to our best estimates for the properties of such melts and/or to the conditions of their interaction with the mantle wedge. Our preference, based on this modeling, is either that slab-derived melts are absent from the mantle sources of the lavas we have studied or, more plausibly, that they are present in such low abundance that they do not contribute significantly either to the bulk $\delta^{18}O$ of melt-generating regions in the sub-arc mantle or to the productivity of melting. This may appear to be inconsistent with recent studies that have concluded that sediment-derived melts (rather than sediment- or basalt-derived hydrous fluids) dominate aspects of the trace element budget of some arc lavas (e.g. Hawkesworth *et al.*, 1997). However, the results of our modeling can be reconciled with trace-element evidence for the importance of slab-derived melts in metasomatism of the mantle wedge if such melts are a minor component of a fluid-dominated slab enrichment of the sub-arc mantle but are sufficiently rich in certain incompatible trace elements that they nevertheless dominate the budgets of those elements.

Concentrations of solutes

To this point, most of the details of the trace-element chemistry of slab-derived metasomatic fluids and/or melts have been unspecified and relatively unimportant to our discussion; that is, the metasomatizing phase has been assumed to be water rich, high in $\delta^{18}O$, and poor in Ti, Cr, HREE, and Sc, and this allowed us to construct models that match our observations. A key feature of this modeling is that it provides estimates of the amounts of slab-derived fluid or melt required in the source regions of studied lavas from the Vanuatu–Fiji–New Caledonia region. These estimates in turn allow us to solve for the abundances of other trace elements in the slab-derived metasomatizing phase that, in the context of our models, are required explain their concentrations in these lavas. In this section, we assume that the metasomatizing phase is the aqueous fluid described previously and solve for its concentrations of a set of minor and trace elements. We emphasize that these calculations are simply logical consequences of the modeling described above and are not framed with the intent of relating our results to recent models of multicomponent slab additions to the mantle wedge (e.g. Elliott *et al.*, 1997).

These calculations are straightforward: a sample's $\delta^{18}O$ value can be used to constrain in the context of our model the total amount of fluid added to its source; that amount of fluid is taken to have driven a total extent of melting given by the batch or fractional curve for solute-rich aqueous fluid in Fig. 5a; partitioning of each element between residue and melt for each increment of melting is calculated using the phase proportions from MELTS, the chosen set of partition coefficients (see the Appendix), and mass balance; and finally, a series of forward calculations are made in which the concentration of each element in the fluid is varied until a match is obtained with the measured abundance in the lava (see the Appendix). The initial mantle source was assumed to have characteristics given in Table 2, as explained above. It should be noted that we solve for only a single slab-derived component for each sample, even though there is evidence for at least two such components in some arcs (Elliott *et al.*, 1997; Fig. 3e and f); if more than one slab-derived component contributes to the trace element budget of the sub-arc mantle, our results can be viewed as a sum of the contributions of all such components divided by the abundance of the aqueous fluid component (i.e. our calculation would systematically overestimate the abundances in the fluid of elements highly concentrated in other components such as slab-derived melts).

We have solved for the required trace element composition of the model aqueous fluid for several samples from the Vanuatu–Fiji–New Caledonia suite. These samples include two island-arc basalts from Vanuatu (one a relatively high-$\delta^{18}O$ lava from Ambrym, Ambrym 28; the other a lower-$\delta^{18}O$ lava from Tongoa, Tongoa-6), one shoshonite from Fiji (E2c), and one boninite from New Caledonia (NC-52). For comparison, we also computed trace element contents of model aqueous flux for an island-arc basalt from Uracas in the Mariana arc (URA-5), although we emphasize that this sample is not part of the Vanuatu–Fiji–New Caledonia suite and thus may not be directly comparable with the fluxed melting model examined in detail in the preceding discussion. The results of these calculations are presented in Fig. 7 as NMORB-normalized compositions of slab-derived fluids calculated for each sample; fluxed-batch-fusion results are presented in Fig. 7a, and fluxed-fractional-fusion results are shown in Fig. 7b. For comparison, we have plotted in Fig. 7c the compositions of the average 'slab' component of McCulloch & Gamble (1991), the 'water-rich component' for the Mariana back-arc from Stolper & Newman (1994), the expected compositions of slab-derived fluids calculated by Brenan *et al.* (1995) based on experimental study of partitioning between solids and fluids and estimated compositions of subducted sediments

and altered basalts, and the expected composition of sediment-derived melt and sediment-derived fluid based on the experiments of Johnson & Plank (1999) and the average composition of sediments subducting into the western Vanuatu trench (Peate *et al.*, 1997; Plank & Langmuir, 1998). It should be noted that absolute concentrations of trace elements in some or all of the samples we have considered may have been modified by fractional crystallization; this could contribute systematic offsets (i.e. shifting the entire pattern up or down in Fig. 7) of tens of percent in the estimated composition of the slab-derived fluid based on any given sample. It also should be noted that to satisfy the concentrations of some HREE of some lavas, calculated concentrations of these elements in the aqueous fluid are required to be negligible; in these cases, reflecting the insensitivity of our model to the slab contribution for these elements, no results are shown in Fig. 7.

The results of our calculations show that the aqueous fluids required by our model are characterized by enrichments in minor and trace elements relative to NMORB that are typically higher for more incompatible elements (i.e. for elements toward the left side of Fig. 7). Superimposed on this general trend are positive anomalies in Rb, Ba (except for the boninite sample), K, and Sr (again nearly absent in the boninite), and a negative anomaly in Nb. These features are typical of arc-related lavas and have been previously inferred to reflect high solubilities of alkali- and alkali-earth elements and low solubilities of HFSE in aqueous fluids (Gill, 1981; McCulloch & Gamble, 1991).

The compositions of fluids calculated assuming a fluxed-fractional-fusion model (Fig. 7b) are similar to one another in their relative abundances of most elements (results for fluxed-batch fusion are only somewhat more scattered). This is particularly true for the four non-boninitic samples. This relatively small range in trace element concentrations of the model fluids, when combined with the success of the model in reproducing the trends in Fig. 4, demonstrates that much of the geochemistry of this group of arc-related lavas can be explained by fluxing the sub-arc mantle with fluids having a small range in oxygen isotope ratios and trace element compositions. The mean composition of these calculated fluids (including the boninite, NC-52) is presented in Table 2 under the heading 'Vanuatu model aqueous fluid'. The fluids calculated assuming a fluxed-batch-fusion model are broadly similar to this composition, the only significant differences being in Y and the middle REE to HREE (see comparison in Fig. 7c).

The calculated trace element composition of the aqueous fluid is similar to that of the H_2O-rich component previously identified as a source of geochemical variability in the source regions of Mariana back-arc lavas [Fig. 7c; note, however, that the H_2O-rich component of Stolper & Newman (1994) is richer in Na and poorer in H_2O than assumed here]. Despite similarities between the models used in this study and by Stolper & Newman (1994) (i.e. both link the abundance of a water-rich component in the source to the extent of melting of that source), the estimates of trace element concentrations in the water-rich components of these two studies are independent, so this is not a necessary or circular result and is therefore encouraging with respect to the robustness of the results of both studies. The success of the fluxed melting model in both cases and the correspondence between the inferred trace-element compositions of the water-rich components in the two studies suggest a similarity between the hydrous component in the Mariana back-arc mantle and the sub-arc mantle sources of several types of lavas from the Vanuatu–Fiji–New Caledonia region. This correspondence is surprising given the expectation that there is not a single, universal slab-derived component (e.g. its composition is expected to vary among different slab-derived components and with the age and sediment stratigraphy of the subducted plate; Elliott *et al.*, 1997; Plank & Langmuir, 1998). It should be emphasized, however, that the patterns compared in Fig. 7 are shown on a logarithmic scale, and there are, in detail, significant differences among the fluid compositions (e.g. the Rb/Ba ratio varies by a factor of 12 among the calculated fluid compositions for different samples shown in Fig. 7).

Although the calculated fluid compositions from this study are similar in terms of trace elements to that inferred by Stolper & Newman (1994), they differ from some other estimates of the composition of such aqueous fluids. For example, the calculated concentrations of Th and U in the slab-derived fluid from this study (for either the batch or fractional melting models) are significantly higher than predicted using known aqueous-fluid–mineral partition coefficients and the estimated composition of typical subducted crust (Brenan *et al.*, 1995). This may be due to natural slab-derived fluids having more 'melt-like' properties with respect to trace element partitioning than do aqueous fluids that have been investigated experimentally (e.g. Shen & Keppler, 1997). Alternatively, the slab-derived components that produced the correlations in Fig. 4 may in fact include contributions from silicate melts that are minor in absolute abundance compared with aqueous fluids but still dominate the budgets of U and Th; such a view of metasomatism of the mantle wedge dominated by aqueous fluids but with contributions from melt has been presented previously (e.g. Moriguti & Nakamura, 1998). Another difference between our results and previous work is that the composition of the slab-derived component given by McCulloch & Gamble (1991), although overlapping for most elements with the range of estimates from this study, is consistently near the low end of the range given here

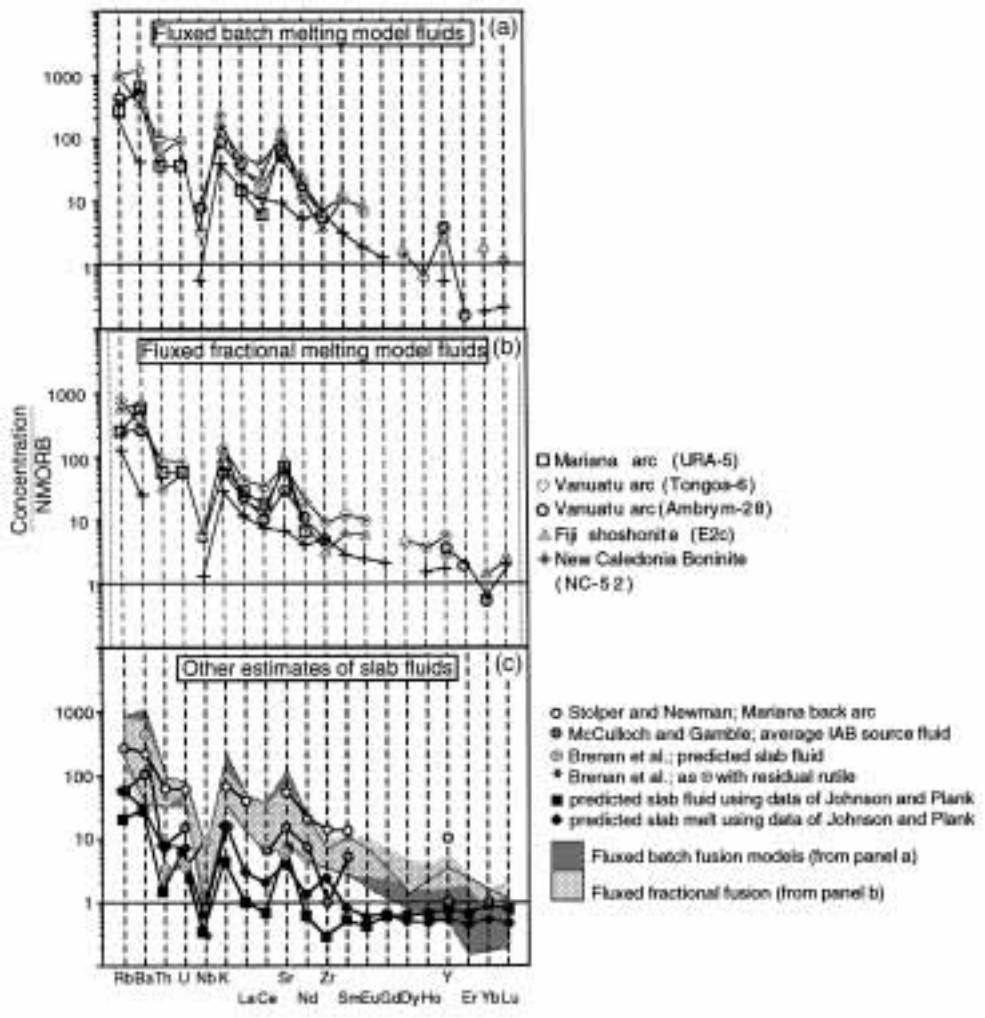

Fig. 7. Calculated concentrations of trace elements in slab-derived aqueous fluid required to satisfy simultaneously the restrictions of fluxed-batch- and fluxed-fractional-fusion models (Fig. 6) and the trace element chemistry of selected lavas considered in this study. (a) Results for fluxed-batch-fusion model; (b) results for fluxed-fractional-fusion model; (c) comparison of ranges of fluid compositions calculated for fluxed-batch- and fluxed-fractional-fusion models with previous estimates of the composition of slab-derived metasomatic components (McCulloch & Gamble, 1991; Stolper & Newman, 1994) or calculated slab-derived melts or fluids based on partition coefficients from Brenan *et al.* (1995) or Johnson & Plank (1999) and assuming equilibrium of an infinitesimal amount of fluid or melt with sediment subducting beneath the Vanuatu arc (Peate *et al.*, 1997). Error bars associated with the estimates of Stolper & Newman [open circles in (c)] are approximately equal to the size of the symbol. (See text and the Appendix for details of the calculations and sources of elemental data on lavas.)

(and some elements, such as Rb, Th, U, and Zr, are more than two times lower than the low end of our range; Fig. 7c). These differences probably reflect a number of factors, but an important one is that McCulloch & Gamble selected a range of 1–5% for the abundance of the slab-derived component in the sub-arc mantle. Our results suggest that the average value is closer to ~0·5–1·0 wt %. Modification of the McCulloch & Gamble model to account for this difference would result in concentrations of most elements in the slab-derived fluid that more closely approach our average estimates. It should be noted that our model slab-derived fluid (and the estimates of McCulloch & Gamble and Stolper & Newman) has higher concentrations of nearly all but the most compatible of trace elements shown in Fig. 7 than is predicted by combining recent experimental results on trace element partitioning for melting or dehydration of sediments (Johnson & Plank, 1999) with the known compositions of sediments subducting beneath the western Vanuatu arc (Peate *et al.*, 1997; filled symbols, Fig. 7c).

The isotopic composition of Sr provides a consistency check on our estimated concentration of Sr in the slab-derived fluid; i.e. if the concentration of Sr arrived at through the preceding exercise is correct, then given reasonable values for the Sr isotope ratios of the slab

and mantle, our model should predict the observed relationship between $\delta^{18}O$ and $^{87}Sr/^{86}Sr$ (Fig. 3a). We have made such a prediction for the suite of island-arc lavas from western Vanuatu (i.e. that subset of Vanuatu lavas erupted adjacent to a portion of the adjacent trench having a well-characterized sedimentary section; Peate *et al.*, 1997). Figure 8 compares our data (black filled circles and triangle for Vanuatu data; gray symbols show data from other locations for comparison) with the trends calculated by our fluid-fluxed melting model (i.e. the mantle and fluid have Sr concentrations listed in Table 2; fluid-fluxed melting follows our model as described above; and the $\delta^{18}O$ of the fluid is as previously assumed for the calculations presented in Fig. 6). We assumed that the mantle wedge initially has an $^{87}Sr/^{86}Sr$ ratio of 0·7027 (comparable with the NMORB source; Ito *et al.*, 1987), that the initial $\delta^{18}O$ of olivine in the source is 5·1‰ (i.e. slightly higher than the value of 5·0‰ in our general model, so that the predicted curve passes through the low-$^{87}Sr/^{86}Sr$ end of the subset of the data being considered), and that the fluid has an $^{87}Sr/^{86}Sr$ ratio between 0·7044 (for altered volcanic rocks) and 0·7072 (for pelagic sediment; both taken from measured values in samples of the slab subducting beneath the western Vanuatu arc; Peate *et al.*, 1997). The resulting calculated curves show that our model slab-derived fluid predicts a strongly hyperbolic covariation of $\delta^{18}O$ and $^{87}Sr/^{86}Sr$, consistent with the observed trend. The value of $^{87}Sr/^{86}Sr$ at which $\delta^{18}O$ values rise sharply is substantially lower than the value of pelagic sediment subducting beneath Vanuatu, requiring in the context of our model that a significant fraction of the Sr in the slab phase is derived from altered volcanic material.

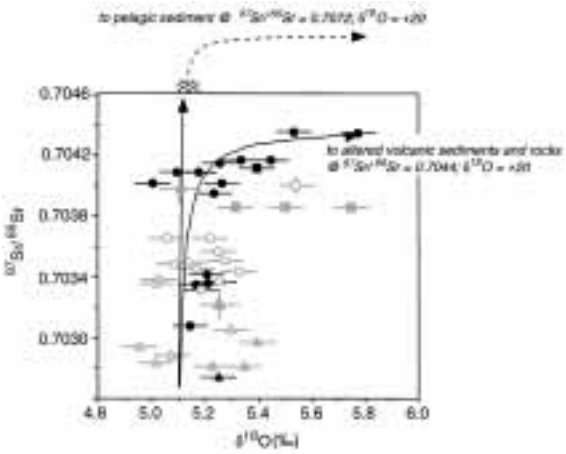

Fig. 8. Comparison of data from Vanuatu (black symbols; gray symbols reproduce other data from Fig. 3a) with calculated trends for our fluxed fusion model assuming that the flux is an aqueous fluid having an Sr concentration equal to the average of the results shown in Fig. 7b (4572 ppm; see Table 2). Two calculated curves are shown representing the extremes in the isotopic composition expected for Sr released from the top of the slab subducting beneath western Vanuatu (Pearce *et al.*, 1998): one assuming that the fluid acquires its Sr from altered volcanoclastic sediments ($^{87}Sr/^{86}Sr$ = 0·7044), the other assuming that Sr is from pelagic sediment ($^{87}Sr/^{86}Sr$ = 0·7072). Batch and fractional models coincide to within the width of the plotted lines. In combination with calculations presented in Figs 6 and 7, this calculation is consistent with the source of Vanuatu lavas being a peridotite similar to the sources of NMORB that has been fluxed by ~0–2 wt % of an aqueous fluid that is high in $\delta^{18}O$, highly enriched in Sr compared with peridotite in the mantle wedge, and in which the Sr is derived principally from altered volcanoclastic sediment (or perhaps from the underlying altered basalt of the oceanic plate, which probably has a similar $^{87}Sr/^{86}Sr$ ratio; Staudigel *et al.*, 1995).

SUMMARY AND CONCLUSIONS

The key observations in this study are the low abundance ($\leq$1%) of crustal oxygen in most (~80%) oceanic arc-related lavas and the relationship between those ^{18}O enrichments that do exist and the integrated extent of melting in the sources of arc-related lavas. This second observation suggests that the extent of melting in the sources of the studied lavas is related to the supply of ^{18}O-enriched, slab-derived oxygen. In our view, the most plausible mechanism for such a relationship is that slab-derived oxygen is introduced as a metasomatic agent into the peridotitic mantle wedge in amounts up to a few percent in the form of a slab-derived aqueous fluid, the abundance or availability of which controls the progress of peridotite melting. This explanation of depleted chemical signatures in arc lavas differs from the widely held view that they reflect a template of variable depletion related to melting in the back-arc environment onto which slab signatures are superimposed in the sub-arc mantle (e.g. Woodhead *et al.*, 1993). The forward model we propose to describe this process can explain quantitatively observed variations in chemistry and $\delta^{18}O$ of lavas from the Vanuatu–Fiji–New Caledonia region, which display the largest range in $\delta^{18}O$ and apparent source fertility of any single suite of related samples examined in this study. We cannot rule out the possibility that this process is driven by hydrous slab melts, but this would require addition of large amounts of slab-derived melt to the mantle wedge, unexpected chemical and isotopic compositions for the hydrous melts, and/or unexpectedly high temperatures in the metasomatized sub-arc mantle wedge (i.e. well above the dry peridotite solidus).

Our interpretation is similar in several of its details to conclusions previously reached through study of the abundances of major and minor elements and water in back-arc-basin and arc basalts and more generally to the widely held notion that slab-derived fluids contribute to both the extent of melting and the chemistry of subduction zone lavas. In particular, Stolper & Newman (1994) and Gribble *et al.* (1998) observed a relationship between the water contents of back-arc-basin basalts in the Mariana

trough and the inferred extent of melting of the sources of those basalts. They concluded that melting in those sources was fluxed by addition to a peridotite similar to the NMORB source of small amounts (typically up to ~0·5 wt %—just below the limit at which an oxygen isotope signal is expected to be seen by our measurements) of a water-rich component having trace element contents similar to those we infer for the agent of fluxed melting in the Vanuatu–Fiji–New Caledonia sub-arc mantle. Crawford *et al.* (1989) proposed that the low CaO/Al_2O_3 ratios and Cr-rich spinels characteristic of boninites reflect derivation from a depleted peridotitic source in the sub-arc mantle that has been melted as a result of fluxing by ~2–3 wt % water. Stern *et al.* (1991) similarly proposed that many aspects of boninite chemistry can be explained by melting a water-rich, highly depleted mantle source. Our results for lavas from the Vanuatu–Fiji–New Caledonia region agree quantitatively with these estimates and serve to link the petrogenesis of these diverse arc-related lavas through a common mechanism. Comparison of our model with samples other than the Vanuatu–Fiji–New Caledonia suite and similar, but more subtle, observations of a relationship between $\delta^{18}O$ and $Na_2O_{(8\cdot0)}$ in a previous study of back-arc lavas from the Lau basin (Macpherson & Mattey, 1997) suggest that this mechanism may be consistent with a wider spectrum of arc-related magmas. However, more specific generalizations must await the discovery of more arc-related suites demonstrating a large range in $\delta^{18}O$ and chemistry.

ACKNOWLEDGEMENTS

We thank Bob Stern for his gracious supply of samples and unpublished data for shoshonites from the Mariana arc. Glen Gaetani, Mike Baker, Ronit Kessel, Peter Wyllie, Bob Stern, and Terry Plank improved upon this work through informal reviews of an early draft of this manuscript and/or helpful discussions on subjects related to this work. We thank Jean Morrison for allowing us to use her laboratory facilities at USC, and Mike Spicuzza and Nami Kitchen for laboratory assistance at the UW and at USC, respectively. A portion of the data presented in this manuscript was collected by Ronit Kessel as part of her graduate studies at Caltech. We gratefully acknowledge the improvements to this manuscript resulting from reviews by Chris Hawkesworth, Peter Kelemen, and Colin Macpherson. This work was supported by NSF Grant EAR-9805101. This is Contribution 8556 of the Division of Geological and Planetary Sciences at the California Institute of Technology.

REFERENCES

Albarède, F. & Michard, A. (1989). Hydrothermal alteration of the oceanic crust. In: Hart, S. R. & Gulen, L. (eds) *Crust/Mantle Recycling at Convergence Zones. NATO ASI Series. Series C: Mathematical and Physical Sciences, 258*. Dordrecht: Kluwer Academic, pp. 29–36.

Arai, S. (1994). Compositional variation of olivine–chromian spinel in Mg-rich magmas as a guide to their residual spinel peridotites. *Journal of Volcanology and Geothermal Research* **59**, 279–293.

Arai, S. & Matsukage, K. (1996). Petrology of the gabbro–troctolite–peridotite complex from Hess Deep, Equatorial Pacific; implications for mantle–melt interaction within the oceanic lithosphere. *Proceedings of the Ocean Drilling Program, Scientific Results 147*. College Station, TX: Ocean Drilling Program, pp. 135–155.

Arthur, M. A., Anderson, T. F. & Kaplan, I. R. (1983). Stable isotopes in sedimentary geology. *Society of Economic Paleontologists and Mineralogists Short Course* **10**, variously paginated.

Baker, M. B., Hirschmann, M. M., Ghiorso, M. S. & Stolper, E. M. (1995). Compositions of near-solidus peridotite melts from experiments and thermodynamic calculations. *Nature* **375**, 308–311.

Bebout, G. E. & Barton, M. D. (1989). Fluid flow and metasomatism in a subduction zone hydrothermal system: Catalina Schist terrane, California. *Geology* **17**, 976–980.

Brenan, J. M., Shaw, H. F., Ryerson, F. J. & Phinney, D. L. (1995). Mineral–aqueous fluid partitioning of trace elements at 900°C and 2·0 GPa: constraints on the trace element chemistry of mantle and deep crustal fluids. *Geochimica et Cosmochimica Acta* **59**, 3331–3350.

Chiba, H., Chacko, T., Clayton, R. N. & Goldsmith, J. R. (1989). Oxygen isotope fractionations involving diopside, forsterite, magnetite and calcite; application to geothermometry. *Geochimica et Cosmochimica Acta* **53**, 2985–2995.

Clayton, R. N. & Mayeda, T. K. (1996). Oxygen isotope studies of achondrites. *Geochimica et Cosmochimica Acta* **60**, 1999–2017.

Clayton, R. N., Onuma, N. & Mayeda, T. K. (1971). Oxygen isotope fractionation in Apollo 12 rocks and soils. *Geochimica et Cosmochimica Acta* **2**, 1417–1420.

Clayton, R. N., Hurd, J. M. & Mayeda, T. K. (1972). Oxygen isotope abundances in Apollo 14 and 15 rocks and minerals. *Lunar Science III. Lunar Science Institute Contribution* **88**, 141–143.

Colson, R. O., McKay, G. A. & Taylor, L. A. (1988). Temperature and composition dependencies of trace element partitioning; olivine/melt and low-Ca pyroxene/melt. *Geochimica et Cosmochimica Acta* **52**, 539–553.

Crawford, A. J., Briqueu, L., Laporte, C. & Hasenaka, T. (1995). Coexistence of Indian and Pacific oceanic upper mantle reservoirs beneath the central New Hebrides island arc. In: Taylor, B. & Natland, J. (eds) *Active Margins and Marginal Basins of the Western Pacific. Geophysical Monograph, American Geophysical Union* **88**, 199–217.

Crawford, A. J., Falloon, T. J. & Green, D. H. (1989). Classification, petrogenesis and tectonic setting of boninites. In: Crawford, A. J. (ed.) *Boninites*. London: Unwin Hyman, pp. 1–49.

Davidson, J. P. & Harmon, R. S. (1989). Oxygen isotope constraints on the petrogenesis of volcanic arc magmas from Martinique, Lesser Antilles. *Earth and Planetary Science Letters* **95**, 255–270.

Defant, M. J. & Drummond, M. S. (1990). Derivation of some modern arc magmas by melting of young subducted lithosphere. *Nature* **347**, 662–665.

DePaolo, D. J. (1981). Trace element and isotopic effects of combined wallrock assimilation and fractional crystallization. *Earth and Planetary Science Letters* **53**, 189–202.

Dick, H. J. B. & Bullen, T. (1984). Chromian spinel as a petrogenetic indicator in abyssal and alpine-type peridotite and spatially associated lavas. *Contributions to Mineralogy and Petrology* **86**, 54–76.

Eggins, S. M. (1993). Origin and differentiation of picritic arc magmas, Ambae (Aoba), Vanuatu. *Contributions to Mineralogy and Petrology* **114**, 79–100.

Eiler, J. M., Farley, K. A., Valley, J. W., Stolper, E. M., Hauri, E. & Craig, H. (1995). Oxygen isotope evidence against bulk recycled sediment in the source of Pitcairn island lavas. *Nature* **377**, 138–141.

Eiler, J. M., Farley, K. A., Valley, J. W., Hauri, E., Craig, H., Hart, S. & Stolper, E. M. (1996). Oxygen isotope variations in ocean island basalt phenocrysts. *Geochimica et Cosmochimica Acta* **61**, 2281–2293.

Eiler, J. M., McInnes, B., Valley, J. W., Graham, C. M. & Stolper, E. M. (1998). Oxygen isotope evidence for slab-derived fluids in the sub-arc mantle. *Nature* **393**, 777–781.

Ellam, R. M. & Hawkesworth, C. J. (1988). Elemental and isotopic variations in subduction related basalts: evidence for a three component model. *Contributions to Mineralogy and Petrology* **98**, 72–80.

Elliott, T., Plank, T., Zindler, A., White, W. & Bourdon, B. (1997). Element transport from slab to volcanic front at the Mariana arc. *Journal of Geophysical Research* **102**, 14991–15019.

Gaetani, G. A. & Grove, T. L. (1998). The influence of water on melting of mantle peridotite. *Contributions to Mineralogy and Petrology* **131**, 323–346.

Garlick, G. D., MacGregor, I. D. & Vogel, D. E. (1971). Oxygen isotope ratios in eclogites from kimberlites. *Science* **172**, 1025–1027.

Garcia, M. O., Muenow, D. W., Kwesi, E. & O'Neil, J. R. (1989). Major element, volatile, and stable isotope geochemistry of Hawaiian submarine tholeiitic glasses. *Journal of Geophysical Research* **94**, 10525–10538.

Garcia, M. O., Ito, E., Eiler, J. M. & Pietruszka, A. J. (1996). Crustal contamination of Kilauea volcano magmas revealed by oxygen isotope analysis of glass and olivine from Puu Oo eruption lavas. *Journal of Petrology* **39**, 803–817.

Ghiorso, M. S., Hirschmann, M. M. & Sack, R. O. (1994). New software models thermodynamics of magmatic systems. *EOS Transactions, American Geophysical Union* **75**, 571–576.

Gill, J. B. (1981). *Orogenic Andesites and Plate Tectonics*. Berlin: Springer-Verlag, 401 pp.

Green, T. H. (1994). Experimental studies of trace-element partitioning applicable to igneous petrogenesis—Sedona 16 years later. *Chemical Geology* **117**, 1–36.

Green, T. H. & Pearson, N. J. (1983). Effect of pressure on rare-earth element partition coefficients in common magmas. *Nature* **305**, 414–416.

Gribble, R. F., Stern, R. J., Newman, S., Bloomer, S. H. & O'Hearn, T. (1998). Chemical and isotopic composition of lavas from the northern Mariana trough: implications for magmagenesis in back-arc basins. *Journal of Petrology* **39**, 125–154.

Harmon, R. S. & Hoefs, J. (1995). Oxygen isotope heterogeneity of the mantle deduced from global ^{18}O systematics of basalts from different geotectonic settings. *Contributions to Mineralogy and Petrology* **120**, 95–114.

Harmon, R. S., Thorpe, R. S. & Francis, P. W. (1981). Petrogenesis of Andean andesites from combined O–Sr isotope relationships. *Nature* **290**, 396–399.

Hart, S. R. & Dunn, T. (1993). Experimental cpx/melt partitioning of 24 trace elements. *Contributions to Mineralogy and Petrology* **113**, 1–8.

Hawkesworth, C. J., O'Nions, R. K., Pankhurst, R. J., Hamilton, P. J. & Evensen, N. M. (1977). A geochemical study of island-arc and back-arc tholeiites from the Scotia sea. *Earth and Planetary Science Letters* **36**, 253–262.

Hawkesworth, C. K., Gallagher, K., Hergt, J. M. & McDermott, F. (1994). Destructive plate margin magmatism: geochemistry and melt generation. *Lithos* **33**, 169–188.

Hawkesworth, C. J., Turner, S. P., McDermott, F., Peate, D. W. & van Calsteren, P. (1997). U–Th isotopes in arc magmas: implications for element transfer from the subducted crust. *Science* **276**, 551–555.

Hawkins, J. W. & Melchior, J. T. (1985). Petrology of Mariana trough and Lau basin basalts. *Journal of Geophysical Research* **90**, 11431–11468.

Hildreth, W. & Moorbath, S. (1988). Crustal contributions to arc magmatism in the Andes of central Chile. *Contributions to Mineralogy and Petrology* **98**, 455–489.

Hirose, K. & Kawamoto, T. (1995). Hydrous partial melting of lherzolite at 1 GPa—the effect of H_2O on the genesis of basaltic magmas. *Earth and Planetary Science Letters* **133**, 463–473.

Hirschmann, M. M. & Stolper, E. M. (1996). A possible role for garnet pyroxenite in the origin of the 'garnet signature' in MORB. *Contributions to Mineralogy and Petrology* **124**, 185–208.

Hirschmann, M. M., Asimow, P. D., Ghiorso, M. S. & Stolper, E. M. (1999). Calculation of peridotite partial melting from thermodynamic models of minerals and melts. III. Controls on isobaric melt production and the effect of water on melt production. *Journal of Petrology* **40**, 831–851.

Hoernes, S. & Friedrichsen, F. (1977). Oxygen isotope investigations of rocks of Leg 37. *Initial Reports of the Deep Sea Drilling Project 37*. Washington, DC: US Government Printing Office, pp. 603–606.

Ito, E. & Stern, R. J. (1985). Oxygen and strontium isotopic investigations of subduction zone volcanism, the case of the Volcano arc and the Marianas island arc. *Earth and Planetary Science Letters* **76**, 312–320.

Ito, E., White, W. M. & Gopel, C. (1987). The O, Sr, Nd and Pb isotope geochemistry of MORB. *Chemical Geology* **62**, 157–176.

Johnson, M. C. & Plank, T. (1999). Dehydration and melting experiments constrain the fate of subducted sediments. *Earth and Planetary Science Letters* (submitted).

Kay, R. W. (1980). Volcanic arc magmas: implications of a melting–mixing model for element recycling in the crust–upper mantle system. *Journal of Geology* **88**, 497–522.

Kelemen, P. B., Johnson, K. T. M., Kinzler, R. J. & Irving, A. J. (1990). High field strength element depletions in arc basalts due to mantle–magma interactions. *Nature* **345**, 521–524.

Kennedy, A. K., Hart, S. R. & Frey, F. A. (1990). Compositional and isotopic constraints on the petrogenesis of alkaline arc lavas; Lihir Island, Papua New Guinea. *Journal of Geophysical Research* **95**, 6929–6942.

Kennedy, A. K., Lofgren, G. E. & Wasserburg, G. J. (1993). An experimental study of trace element partitioning between olivine, orthopyroxene and melt in chondrules: equilibrium values and kinetic effects. *Earth and Planetary Science Letters* **115**, 177–195.

Keppler, H. (1996). Constraints from partitioning experiments on the composition of subduction-zone fluids. *Nature* **380**, 237–240.

Klein, E. M. & Langmuir, C. H. (1987). Global correlations of ocean ridge basalt chemistry with axial depth and crustal thickness. *Journal of Geophysical Research* **92**, 8089–8115.

Kolodny, Y. & Epstein, S. (1976). Stable isotope geochemistry of deep sea cherts. *Geochimica et Cosmochimica Acta* **40**, 1195–1209.

Kushiro, I. (1975). On the nature of silicate melt and its significance in magma genesis: regularities in the shift of the liquidus boundaries involving olivine, pyroxene, and silica minerals. *American Journal of Science* **275**, 411–431.

Kushiro, I., Syono, Y. & Akimoto, S. (1968). Melting of a peridotite nodule at high pressures and high water pressures. *Journal of Geophysical Research* **73**, 6023–6029.

Kyser, T. K., O'Neil, J. R. & Carmichael, I. S. E. (1981). Oxygen isotope thermometry of basic lavas and mantle nodules. *Contributions to Mineralogy and Petrology* **77**, 11–23.

Kyser, T. K., O'Neil, J. R. & Carmichael, I. S. E. (1982). Genetic relations among basic lavas and ultramafic nodules: evidence from oxygen isotope compositions. *Contributions to Mineralogy and Petrology* **81**, 88–102.

Leeman, W. P., Carr, M. J. & Morris, J. D. (1994). Boron geochemistry of the Central American volcanic arc: constraints on the genesis of subduction-related magmas. *Geochimica et Cosmochimica Acta* **58**, 149–168.

Lin, P. N., Stern, R. J. & Bloomer, S. H. (1989). Shoshonitic volcanism in the northern Mariana arc, 2, Large-ion lithophile and rare earth element abundances: evidence for the source of incompatible element enrichments in intraoceanic arcs. *Journal of Geophysical Research* **94**, 4497–4514.

Macpherson, C. G. & Mattey, D. P. (1997). Oxygen isotope variations in Lau Basin lavas. *Chemical Geology* **144**, 177–194.

Macpherson, C. G., Gamble, J. A. & Mattey, D. P. (1998). Oxygen isotope geochemistry of lavas from an oceanic to continental arc transition, Kermadec–Hikurangi margin, SW Pacific. *Earth and Planetary Science Letters* **160**, 609–621.

Maillet, P., Monzier, M. & Leferve, C. (1986). Petrology of Matthew and Hunter volcanoes, south New Hebrides island arc (southwest Pacific). *Journal of Volcanology and Geothermal Research* **30**, 1–27.

Matsuhisa, Y., Matsubaya, O. & Sakai, H. (1973). Oxygen isotope variations in magmatic differentiation processes of the volcanic rocks in Japan. *Contributions to Mineralogy and Petrology* **39**, 277–288.

Mattey, D., Lowry, D. & Macpherson, C. (1994). Oxygen isotope composition of mantle peridotite. *Earth and Planetary Science Letters* **128**, 231–241.

Matthews, A., Stolper, E. M., Eiler, J. M. & Epstein, S. (1998). Oxygen isotope fractionation among melts, minerals and rocks. In: *1998 Goldschmidt Conference, Toulouse*. London: Mineralogical Society, pp. 971–972.

McCulloch, M. T. & Gamble, J. A. (1991). Geochemical and geodynamical constraints on subduction zone magmatism. *Earth and Planetary Science Letters* **102**, 358–374.

McKenzie, D. & O'Nions, R. K. (1995). The source regions of ocean island basalts. *Journal of Petrology* **36**, 133–159.

Michael, P. (1995). Regionally distinctive sources of depleted MORB: evidence from trace elements and H_2O. *Earth and Planetary Science Letters* **131**, 301–320.

Monzier, M., Danyushevsky, L. V., Crawford, A. J., Bellon, H. & Cotten, J. (1993). High-Mg andesites from the southern termination of the New Hebrides island arc (SW Pacific). *Journal of Volcanology and Geothermal Research* **57**, 193–217.

Moriguti, T. & Nakamura, E. (1998). Across-arc variation of Li isotopes in lavas and implications for crust/mantle recycling at subduction zones. *Earth and Planetary Science Letters* **163**, 167–174.

Morris, J. & Tera, F. (1989). ^{10}Be and ^{9}Be in mineral separates and whole rocks from volcanic arcs: implications for sediment subduction. *Geochimica et Cosmochimica Acta* **53**, 3197–3206.

Muehlenbachs, K. (1986). Alteration of the oceanic crust and the ^{18}O history of seawater. In: Valley, J. W., Taylor, H. P. & O'Neil, J. R. (eds) *Stable Isotopes in High Temperature Geological Processes, Vol. 16*. Washington, DC: Mineralogical Society of America, pp. 425–444.

Muehlenbachs, K. & Kushiro, I. (1974). Oxygen isotope exchange and equilibrium of silicates with CO_2 or O_2. *Carnegie Instution of Washington Yearbook* **71**, 232–236.

Nichols, G. T., Wyllie, P. J. & Stern, C. R. (1994). Subduction zone melting of pelagic sediments constrained by melting experiments. *Nature* **371**, 785–788.

Nielsen, R. L., Forsythe, L. R. & Fisk, M. R. (1993). The partitioning of HFSE between magnetite and natural mafic to intermediate liquids at low pressure. *EOS Transactions, American Geophysical Union* **74**, 338–339.

Nielsen, R. L., Gallahan, W. E. & Newberger, F. (1994). Experimentally determined mineral–melt partition coefficients for Sc, Y and REE for olivine, orthopyroxene, pigeonite, magnetite and ilmenite. *Contributions to Mineralogy and Petrology* **110**, 488–499.

O'Neil, J. R. & Taylor, H. P. (1967). The oxygen isotope and cation exchange chemistry of feldspars. *American Mineralogy* **52**, 1414–1437.

Onuma, N., Clayton, R. N. & Mayeda, T. K. (1970). Oxygen isotope fractionation between minerals and an estimate of the temperature of formation. *Science* **167**, 536–538.

Palin, J. M., Epstein, S. & Stolper, E. M. (1996). Oxygen isotope partitioning between rhyolitic glass/melt and CO_2: an experimental study at 550–950°C and 1 bar. *Geochimica et Cosmochimica Acta* **60**, 1963–1973.

Peacock, S. M. (1996). Thermal and petrologic structure of subduction zones. In: Bebout, G. E., Scholl, D. W., Kirby, S. H. & Platt, J. P. (eds) *Subduction Top to Bottom. Geophysical Monograph, American Geophysical Union* **96**, 119–133.

Pearce, J. A., Baker, P. E., Harvey, P. K. & Luff, I. W. (1995). Geochemical evidence for subduction fluxes, mantle melting and fractional crystallization beneath the South Sandwich island arc. *Journal of Petrology* **36**, 1073–1109.

Peate, D. W., Pearce, J. A., Hawkesworth, C. J., Colley, H., Edwards, C. M. H. & Hirose, K. (1997). Geochemical variations in Vanuatu arc lavas: the role of subducted material and a variable mantle wedge composition. *Journal of Petrology* **38**, 1331–1358.

Pineau, F., Javoy, M., Hawkins, J. W. & Craig, H. (1976). Oxygen isotopic variations in marginal basin and ocean-ridge basalts. *Earth and Planetary Science Letters* **28**, 299–307.

Plank, T. & Langmuir, C. H. (1988). An evaluation of the global variations in the major element chemistry of arc basalts. *Earth and Planetary Science Letters* **90**, 349–370.

Plank, T. & Langmuir, C. H. (1993). Tracing trace elements from sediment input to volcanic output at subduction zones. *Nature* **362**, 739–743.

Plank, T. & Langmuir, C. H. (1998). The chemical composition of subducting sediment and its consequences for the crust and mantle. *Chemical Geology* **145**, 325–394.

Reddy, K. P. R., Oh, S. M., Major, L. D. & Cooper, A. R. (1980). Oxygen diffusion in forsterite. *Journal of Geophysical Research* **85**, 322–326.

Regelous, M., Collerson, K. D., Ewart, A. & Wendt, J. I. (1997). Trace element transport rates in subduction zones: evidence from Th, Sr and Pb isotope data for Tonga–Kermadec arc lavas. *Earth and Planetary Science Letters* **150**, 291–302.

Rogers, N. W. & Setterfield, T. N. (1994). Potassium and incompatible-element enrichment in shoshonitic lavas from the Tavua volcano, Fiji. *Chemical Geology* **118**, 43–62.

Rosenbaum, J. M. (1994). Stable isotope fractionation between carbon dioxide and calcite at 900°C. *Geochimica et Cosmochimica Acta* **58**, 3747–3753.

Ryan, J. F., Morris, J., Tera, F., Leeman, W. P. & Tsvetkov, A. (1995). Cross-arc geochemical variations in the Kurile arc as a function of slab depth. *Science* **270**, 625–627.

Saunders, A. D. & Tarney, J. (1979). The geochemistry of basalts from a back-arc spreading centre in the East Scotia Sea. *Geochimica et Cosmochimica Acta* **43**, 555–572.

Schiano, P., Clocchiatti, R., Shimizu, N., Maury, R. C., Jochum, K. P. & Hofmann, A. W. (1995). Hydrous, silica-rich melts in the sub-arc mantle and their relationship with erupted arc lavas. *Nature* **377**, 595–600.

Schneider, M. E. & Eggler, D. H. (1986). Fluids in equilibrium with peridotite minerals: implications for mantle metasomatism. *Geochimica et Cosmochimica Acta* **50**, 711–724.

Sharma, M., Wasserburg, G. J., Papanastassiou, D. A., Quick, J. E., Sharkov, E. V. & Laz'ko, E. E. (1997). High ^{143}Nd/^{144}Nd in extremely

depleted mantle rocks. *Earth and Planetary Science Letters* **135**, 101–114.

Shen, A. H. & Keppler, H. (1997). Direct observation of complete miscibility in the albite–H_2O system. *Nature* **385**, 710–712.

Shimizu, N. & Arculus, R. J. (1975). Rare earth element concentrations in a suite of basanitoids and alkali olivine basalts from Grenada, Lesser Antilles. *Contributions to Mineralogy and Petrology* **50**, 231–240.

Sigurdsson, I. A., Kamenetsky, V. S., Crawford, A. J., Eggins, S. M. & Zlobin, S. K. (1993). Primitive island arc and oceanic lavas from the Hunter ridge–Hunter fracture zone. Evidence from glass, olivine and spinel compositions. *Mineralogy and Petrology* **47**, 149–169.

Singer, B. S., O'Neil, J. R. & Brophy, J. G. (1992). Oxygen isotope constraints on the petrogenesis of Aleutian arc magmas. *Geology* **20**, 367–370.

Smith, T. E., Thirlwall, M. F. & Macpherson, C. (1996). Trace element and isotope geochemistry of the volcanic rocks at Bequia, Grenadine islands, Lesser Antilles arc: a study of subduction enrichment and intra-crustal contamination. *Journal of Petrology* **37**, 117–143.

Staudigel, H., Davies, G. R., Hart, S. R., Marchant, K. M. & Smith, B. M. (1995). Large scale isotopic Sr, Nd and O isotopic anatomy of altered oceanic crust: DSDP/ODP sites 417/418. *Earth and Planetary Science Letters* **130**, 169–185.

Stern, R. J., Morris, J., Bloomer, S. H. & Hawkins, J. W. (1991). The source of the subduction component in convergent margin magmas: trace element and radiogenic isotope evidence from Eocene boninites, Mariana forearc. *Geochimica et Cosmochimica Acta* **55**, 1467–1481.

Stolper, E. M. & Newman, S. (1994). The role of water in the petrogenesis of Mariana trough magmas. *Earth and Planetary Science Letters* **121**, 293–325.

Sun, S. S. & Nesbitt, R. W. (1979). Geochemical characteristics of mid-ocean ridge basalts. *Earth and Planetary Science Letters* **44**, 119–138.

Sun, S. S. & McDonough, W. F. (1989). Chemical and isotopic systematics of oceanic basalts: implications for mantle composition and processes. In: Saunders, A. D. & Norry, M. J. (eds) *Magmatism in the Ocean Basins*. *Geological Society, London, Special Publications* **42**, 313–345.

Taylor, H. P., Jr (1986). Igneous rocks: I. Processes of isotopic fractionation and isotope systematics. In: Valley, J. W., Taylor, H. P. & O'Neil, J. R. (eds) *Stable Isotopes in High Temperature Geological Processes, Vol. 16*. Washington, DC: Mineralogical Society of America, pp. 227–272.

Thirlwall, M. F., Graham, A. M., Arculus, R. J., Harmon, R. S. & Macpherson, C. G. (1996). Resolution of the effects of crustal assimilation, sediment subduction, and fluid transport in island arc magmas: Pb–Sr–Nd–O isotope geochemistry of Grenada, Lesser Antilles. *Geochimica et Cosmochimica Acta* **60**, 4785–4810.

Toramaru, A. & Fujii, N. (1984). Connectivity of melt phase in a partially molten peridotite. *Journal of Geophysical Research* **91**, 9239–9252.

Turner, S., Hawkesworth, C., Rogers, N., Bartlett, J., Worthington, T., Hergt, J., Pearce, J. & Smith, I. (1997). ^{238}U–^{230r}Th disequilibria, magma petrogenesis, and flux rates beneath the depleted Tonga–Kermadec island arc. *Geochimica et Cosmochimica Acta* **61**, 4855–4884.

Valley, J. W., Kitchen, N., Kohn, M. J., Niendorff, C. R. & Spicuzza, M. J. (1995). Strategies for high precision oxygen isotope analysis by laser fluorination. *Geochimica et Cosmochimica Acta* **59**, 5223–5231.

Woodhead, J. D., Harmon, R. S. & Fraser, D. G. (1987). O, S, Sr, and Pb isotope variations in volcanic rocks from the northern Mariana islands; implications for crustal recycling in intra-oceanic arcs. *Earth and Planetary Science Letters* **83**, 39–52.

Woodhead, J., Eggins, S. & Gamble, J. (1993). High field strength and transition element systematics in island arc and backarc basin basalts: evidence for multi-phase melt extraction and a depleted mantle wedge. *Earth and Planetary Science Letters* **114**, 491–504.

APPENDIX

Calculated concentrations of trace- and minor-element solutes in the slab-derived fluid were made as follows. The concentration of a given element in a lava produced by fluxed batch fusion is described by the equation

$$C_l = [C_s(1 - X_{fl}) + X_{fl}C_{fl}]/[(1\text{-}F)D + F] \quad \text{(A1)}$$

where X_{fl} is based on the $\delta^{18}O$ of olivine in the lava, the estimated $\delta^{18}O$ of our slab and mantle end members, and the contrast in oxygen concentration between peridotite and water. Values of F are based on estimates of X_{fl} and the MELTS-derived relationship between F and X_{fl} (Fig. 5a). C_s is the initial concentration of the element of interest in peridotite before any addition of a slab phase (Table 2), and C_l is the concentration of the element of interest measured in the lava. Equation (A1) is for batch melting, modified for addition of the aqueous slab component to the initial source. Solid–melt distribution coefficients were taken from several sources (Table A1). The bulk partition coefficient is based on the mineralogy of the residue as generated by our MELTS calculations. Fractional melting calculations were made similarly, but the process was broken into steps in which a small amount of slab fluid (X_{fl} = 0·0005) was added to the initial peridotite source and a small extent of melting (F = 0·005–0·01) proceeded as modeled by MELTS (Fig. 5a). The increment of melt was then removed and the residue used as the initial source for the next step. This calculation closely approaches the analytical solution for perfect fractional fusion for elements not supplied by the slab-derived fluid phase.

The calculation of the *cr*-number of chromite was treated somewhat differently. The experiments of Hirose & Kawamoto (1995) were used to constrain the dependence of the distribution coefficient for Al on the extent of melting and the relationship between the *cr*-number of the residue and the *cr*-number of chromite in the residue. Cr was assumed to be a compatible element (D_{bulk} = 10; Dick & Bullen, 1984). Results of the MELTS algorithm include calculated *cr*-numbers of residual spinel and agree qualitatively with the results of this treatment, but are systematically offset from the plotted model curves in Fig. 6a, reflecting the absence of Cr in pyroxene in the MELTS model.

Table A1: Mineral–melt distribution coefficients used in this study

	Ol	CPX	OPX	Spinel
K	0·00005	0·0072	0·0001	0·001
Rb	0·00001	0·002	0·0001	*0·002*
Ba	0·0003	0·00068	0·0001	*0·0005*
Sr	0·0015	0·13	0·0005	*0·1*
La	0·00003	0·054	0·00005	0·003
Ce	0·0001	0·09	0·00015	*0·003*
Nd	0·0004	0·15	0·0005	0·005
Sm	0·001	0·25	0·0015	0·0075
Eu	0·0008	0·3	0·0007	0·006
Gd	0·001	0·36	0·006	0·006
Dy	0·001	0·4	0·008	*0·008*
Ho	*0·005*	0·45	0·01	0·008
Er	0·01	0·45	0·015	0·004
Yb	0·035	0·91	0·214	0·007
Lu	0·04	0·43	0·04	0·023
Y	0·01	0·4	0·01	*0·023*
Th	0·00005	0·013	0·0001	*0·01*
U	0·00002	0·0038	0·0002	*0·01*
Zr	0·0007	0·123	0·014	0·4
Nb	0·00004	0·0077	0·002	0·4
Ti	0·032	0·358	0·215	0·167
Sc	0·2	1·5	0·6	0·05
Cr	*Bulk* D = *10; Dick & Bullen (1994)*			
Al	*D* parameterized as function of *F* using data of Hirose & Kawamoto (1995)			

Italics indicate an estimate based on interpolation between elements having similar compatibility by the classification of Green (1994). Data of Green & Pearson (1983); Colson *et al.* (1988), Keleman et al. (1990), Hart & Dunn (1993), Kennedy *et al.* (1993), Nielsen *et al.* (1993, 1994), and Green (1994).